CHAPTER 4: RESULTS
ALTERED GENE EXPRESSION IN OXYGEN-INDUCED RETINOPATHY

4.1 ABSTRACT

The differential susceptibility to OIR exhibited by two albino inbred rat strains is likely to result in changes in retinal gene expression between these strains. Whilst many genes involved in the angiogenic response to hypoxia have previously been implicated in the pathogenesis of OIR, none of these genes has been found to contribute directly to differential susceptibility to the disease. Affymetrix microarrays were used to analyse the differential expression of over 27,000 genes in response to cyclic hyperoxia in F344 (resistant to OIR) and SD (susceptible to OIR) rats. Three genes, EGLN3, EGLN1 and IGFBP3, were found to be differentially expressed in a strain-dependent manner in response to relative hypoxia. EGLN3 and EGLN1 are involved in the regulation of the HIF-α oxygen sensing pathway and dysregulation of this pathway in SD rats may contribute to susceptibility to OIR. Low expression of IGFBP3 has previously been associated with impaired retinal vascularisation and persistent vaso-obliteration and may account for the presence of large retinal avascular areas, a sign of susceptibility to OIR in SD rats.

4.1a Introduction

Changes in retinal gene expression are likely to underlie the differential susceptibility to OIR that is exhibited by F344 and SD rats. Previous studies in rodent models of OIR identified a number of genes that were differentially

expressed in response to hyperoxia, including VEGF and PEDF which are known to be involved in angiogenesis and retinal vascularisation [98, 100, 212]. Insulin-like growth factor-1 (IGF-1), a growth factor critical for normal foetal growth and development also plays a major role in normal vascularisation of the human retina [20, 224].

4.1.a.1 HIF-α and the response to hypoxia

The induction of the angiogenic response to hypoxia is mediated by the hypoxia-inducible factor HIF, a master transcription factor thought to play a role in regulating oxygen-dependent diseases in the retina [8, 35]. Activated HIF binds to the hypoxia response element (HRE) in the promoter of target genes such as VEGF to induce their upregulation in response to hypoxia (Figure 4.1a) [34, 35, 45]. In normoxia, HIF-α levels are regulated by two classes of oxygen-dependent hydroxylases, which either prevent the recruitment of co-activators required for activation (asparaginyl hydroxylases; FIH) or target HIF-α for polyubiquitination and proteasomal degradation (prolyl hydroxylases; PHD; Figure 4.1b) [43, 53]. Perturbations in the oxygen sensing pathway may have down-stream consequences for HIF-induced regulation of gene expression, and contribute to differences in susceptibility to OIR.

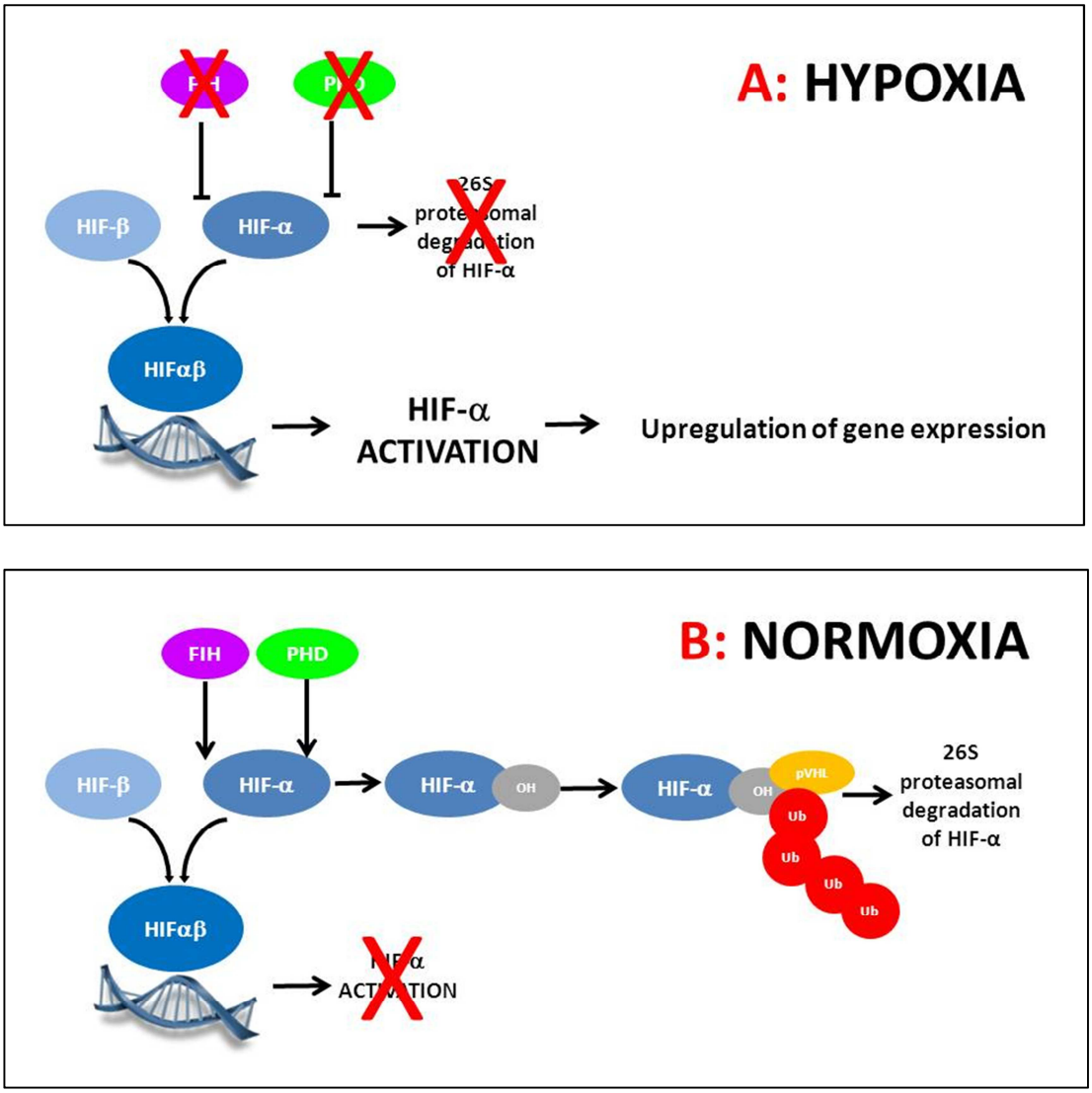

Figure 4.1 (A) Simplified schematic representation of the HIF-α oxygen sensing pathway in hypoxic conditions. In hypoxic conditions, the activity of the oxygen-dependent hydroxylases FIH and PHD are limited, therefore HIF-α accumulates. HIF-α is then able to bind to the constitutively expressed HIF-β subunit and promote the recruitment of co-activators required for HIF-α activation. HIF-α is then able to bind to the hypoxia response element in the promoter of target genes to induce gene expression. **(B) Simplified schematic representation of the HIF-α oxygen sensing pathway in normoxic conditions**. In normoxic conditions, 2 classes of oxygen-dependent hydroxylases regulate the expression of HIF-α. FIH an asparginyl hydroxylase prevents the recruitment of co-activators required for HIF-α activation. PHD on the other hand hydroxylates specific proline residues on HIF-α to target it for polyubiquitination and subsequent proteasomal degradation. Ub = Ubiquitin; PHD = Prolyl hydroxylase domain protein; FIH = Factor inhibiting HIF (Asparaginyl hydroxylase domain protein); pVHL = von Hippel Lindau protein.

4.1.a.2 Specific aims and overview of approach

The specific aims of this chapter were to investigate changes in retinal mRNA expression in two strains of rats which differ in their response to oxygen therapy, and to determine at which time point these changes were occurring.

Microarrays were used to investigate changes in gene expression as they offer a high-throughput screening approach to investigate the differential expression of hundreds to tens of thousands of genes within a sample simultaneously [225, 226]. A microarray-based approach has advantages over a candidate gene approach that is normally limited to a small number of pre-determined genes, as microarrays provide a snapshot of global gene expression changes without making assumptions about the relevance of each gene to the condition being investigated.

Affymetrix microarrays were used to identify genes which were differentially expressed in a strain-dependent manner and/or were regulated by oxygen. Quantitative real-time reverse transcription-polymerase chain reaction (real-time RT-PCR) provided a sensitive method for the quantification of candidate genes and was used to validate microarray findings [227]. Additional genes of interest which had previously been associated with OIR/ROP were also investigated.

4.2 AFFYMETRIX MICROARRAY RESULTS

Affymetrix microarrays were performed using pooled RNA samples from the neural retina (with the RPE attached) of F344 room air-exposed (FRA), F344 cyclic hyperoxia-exposed (FO_2), SD room air-exposed (SDRA) and SD cyclic hyperoxia-exposed (SDO_2) rats, at postnatal days 3, 5 and 6. Each pool consisted of 3 rats of the same strain and treatment, from a minimum of 2 different litters. Examining changes in gene expression at days 3, 5 and 6 enabled identification of changes which were specific to hyperoxia at days 3 and 5 or to relative hypoxia at day 6. Early time points within the cyclic hyperoxia exposure protocol were chosen as changes in gene expression occurring at these time points may provide insight into the causation of the phenotype. In contrast, the changes in gene expression occurring at day 14, when OIR is well established, may be a consequence of the initial changes at the early time points and may not necessarily be causative of OIR. Changes in retinal vascular phenotype in response to cyclic hyperoxia are observed as early as postnatal day 3, as shown in Figure 4.2.

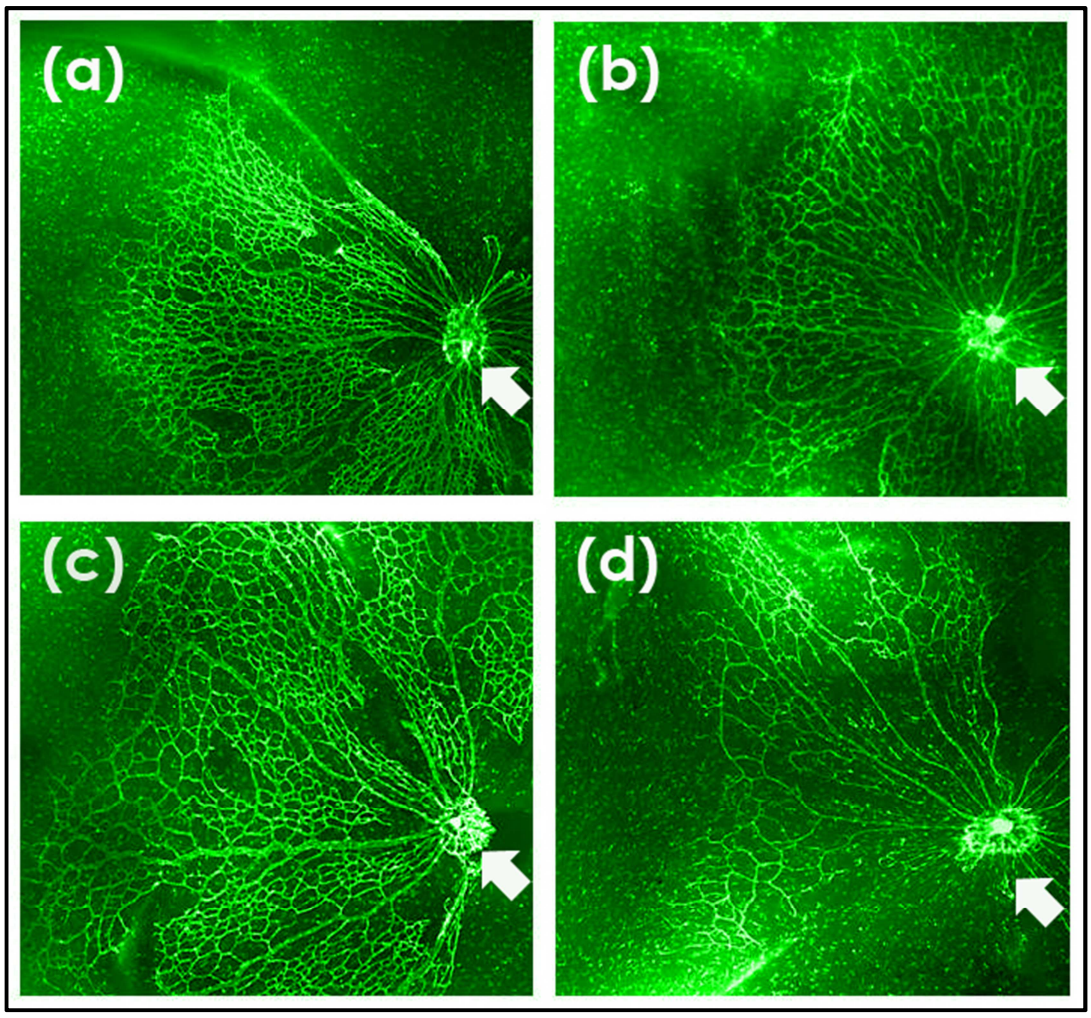

Figure 4.2 Montages of representative sectors of retinae of room air-exposed and cyclic hyperoxia-exposed rats at postnatal day 3 and labelled with fluorochrome-conjugated GS-IB4 to highlight the vasculature. (a) F344 rat raised in room air; (b) F344 rat exposed to cyclic hyperoxia from birth; (c) SD rat raised in room air; (d) SD rat exposed to cyclic hyperoxia from birth. During normal retinal vascular development, vessels develop from the optic nerve head (indicated by arrow) towards the peripheral retina. At postnatal day 3, vessels in the room air-exposed and cyclic hyperoxia-exposed F344 rats, and in the room air-exposed SD rats, had begun to develop and showed normal morphology (a–c). SD rats exposed to cyclic hyperoxia showed aberrant vascular development, with fewer vessels radiating from the optic nerve head and reduced density of the capillary network (d).

4.2.a Statistical analysis of microarray data

Processing of Affymetrix raw gene array data and principal components analyses were performed by Mark van der Hoek (Adelaide Microarray Centre, Adelaide, Australia) using Partek Genomics Suite software. Differential gene expression was assessed by ANOVA, with the p value adjusted using step-up multiple test correction to control the false discovery rate (FDR). The FDR was set to a significance level of 0.05 and represented the number of false positives that may be present within the dataset. Adjusted p values <0.05 were considered to be significant. Over 27, 000 genes were analysed at each time point. Four different comparisons were made to determine whether changes in gene expression were due to strain or oxygen exposure or both (Table 4.1).

Comparison	**Differential gene expression association**
FRA vs. SDRA	Strain-related
FO_2 vs. FRA	Oxygen-related differences in F344 rats resistant to OIR
SDO_2 vs. SDRA	Oxygen-related differences in SD rats susceptible to OIR
FO_2 vs. SDO_2	Differences associated with strain AND cyclic hyperoxia exposure

Table 4.1 Affymetrix microarray comparisons performed at days 3, 5 and 6. Four different comparisons were made to identify differences in gene expression associated with strain, oxygen exposure or both. Differences due to strain and oxygen were of greatest interest. FRA = F344 room air-exposed; SDRA = SD room air-exposed; FO_2 = F344 cyclic hyperoxia-exposed; SDO_2 = cyclic hyperoxia-exposed.

4.2.a.1 Principal Components Analysis of microarray data

Initially, two total RNA samples were provided for each of the 4 experimental conditions (F344 room-air exposed, F344 cyclic hyperoxia-exposed, SD room air-exposed, SD cyclic hyperoxia-exposed). Sample grouping of the corrected data was assessed using a Principal Component Analysis (PCA) plot (Partek Genomics Suite) at each time point. Preliminary PCA analysis of day 3 samples showed large variation in the second principal component for samples from F344 cyclic hyperoxia-exposed (FO_2) rats and variation in the first principal component for samples from SD room air-exposed (SDRA) rats (Figure 4.3). As a result, additional samples for FO_2 and SDRA rats were submitted for analysis. The enhanced data set at day 3 was re-analysed by PCA as shown in Figure 4.4.

PCA was also performed on samples from days 5 and 6 (Figure 4.5). All samples were considered to group in an acceptable manner to be included in the overall analysis of mRNA expression.

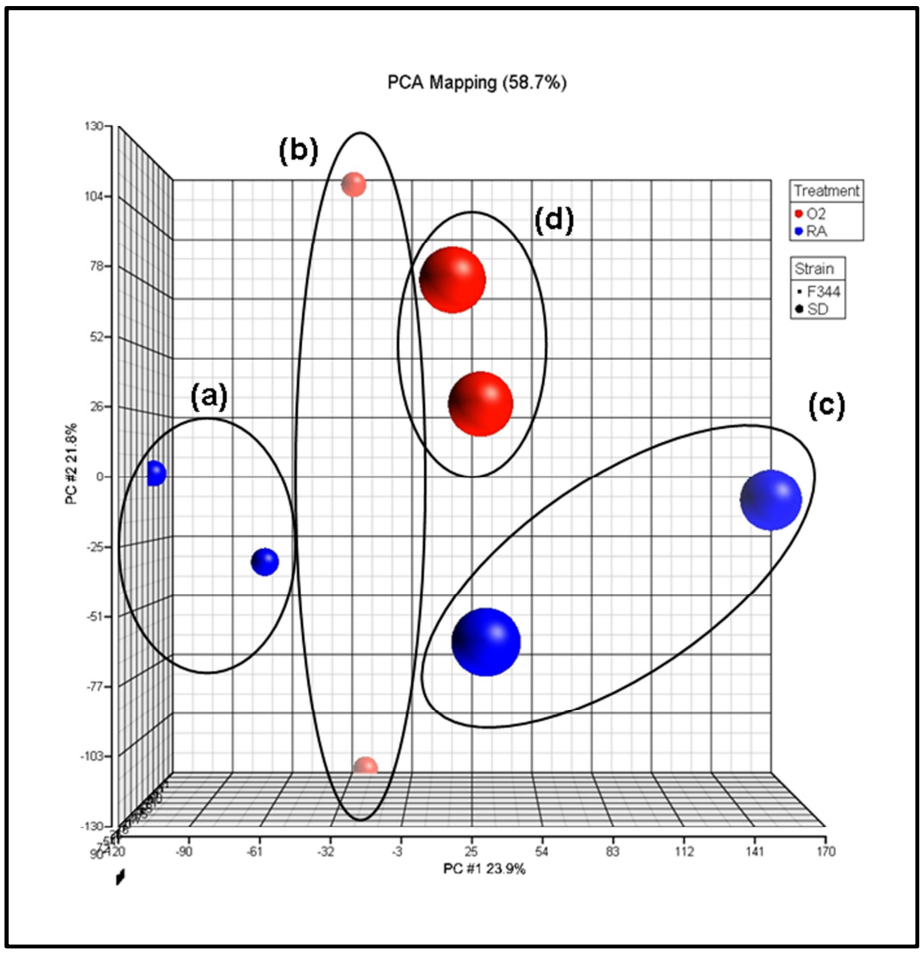

Figure 4.3 Principal component analysis of day 3 samples (n=2). (a) F344 rats raised in room air, (b) F344 rats exposed to cyclic hyperoxia from birth, (c) SD rats raised in room air, (d) SD rats exposed to cyclic hyperoxia from birth. Samples clustered according to strain and exposure with cyclic hyperoxia. A large variation was seen in the second principal component in (b). Variation was also seen in the first principal component in (c). As a result, a third pool of RNA was submitted for analysis for these two experimental conditions.

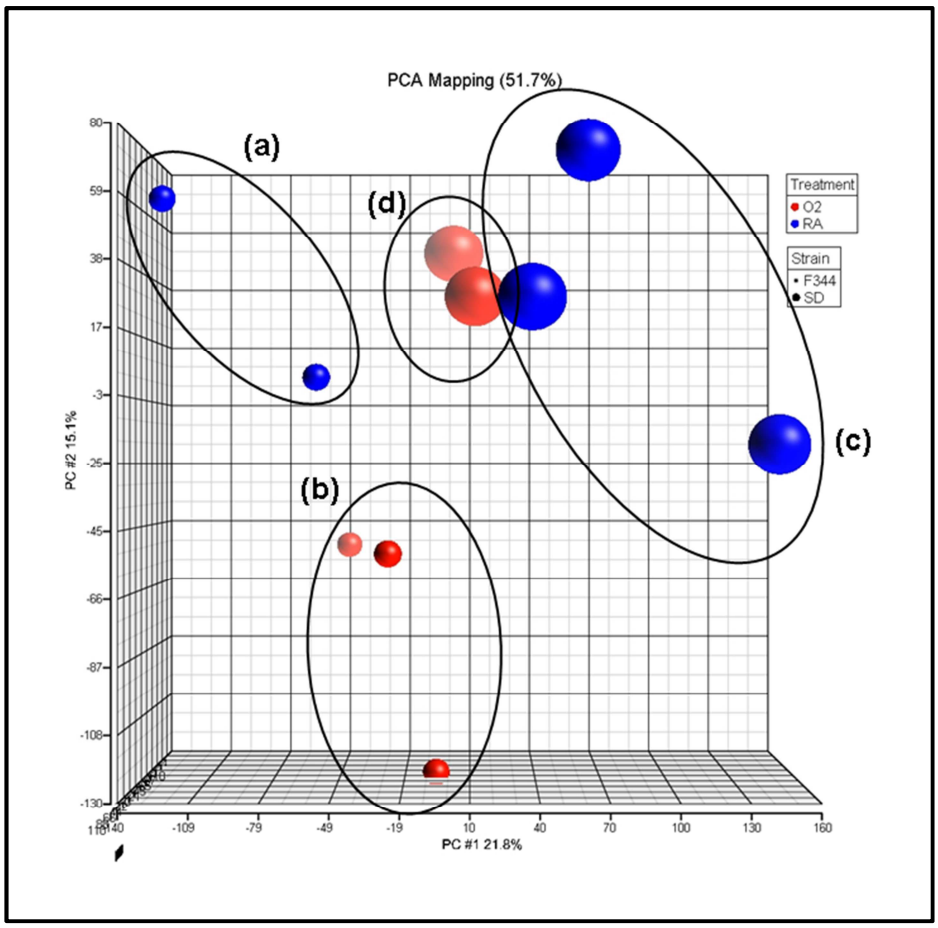

Figure 4.4 Principal component analyses of original and additional day 3 samples corrected for batch variation as a result of two separate sample runs. (a) F344 rats raised in room air (n=2), (b) F344 rats exposed to cyclic hyperoxia from birth (n=3), (c) SD rats raised in room air (n=3), (d) SD rats exposed to cyclic hyperoxia from birth (n=2). Samples clustered according to strain but not by exposure to cyclic hyperoxia with the additional samples. Reduced variation in principal component two was seen in (b). The variation in principal component one for (c) also decreased. Additional samples were considered to group in an acceptable manner to be included in the overall analysis of mRNA expression.

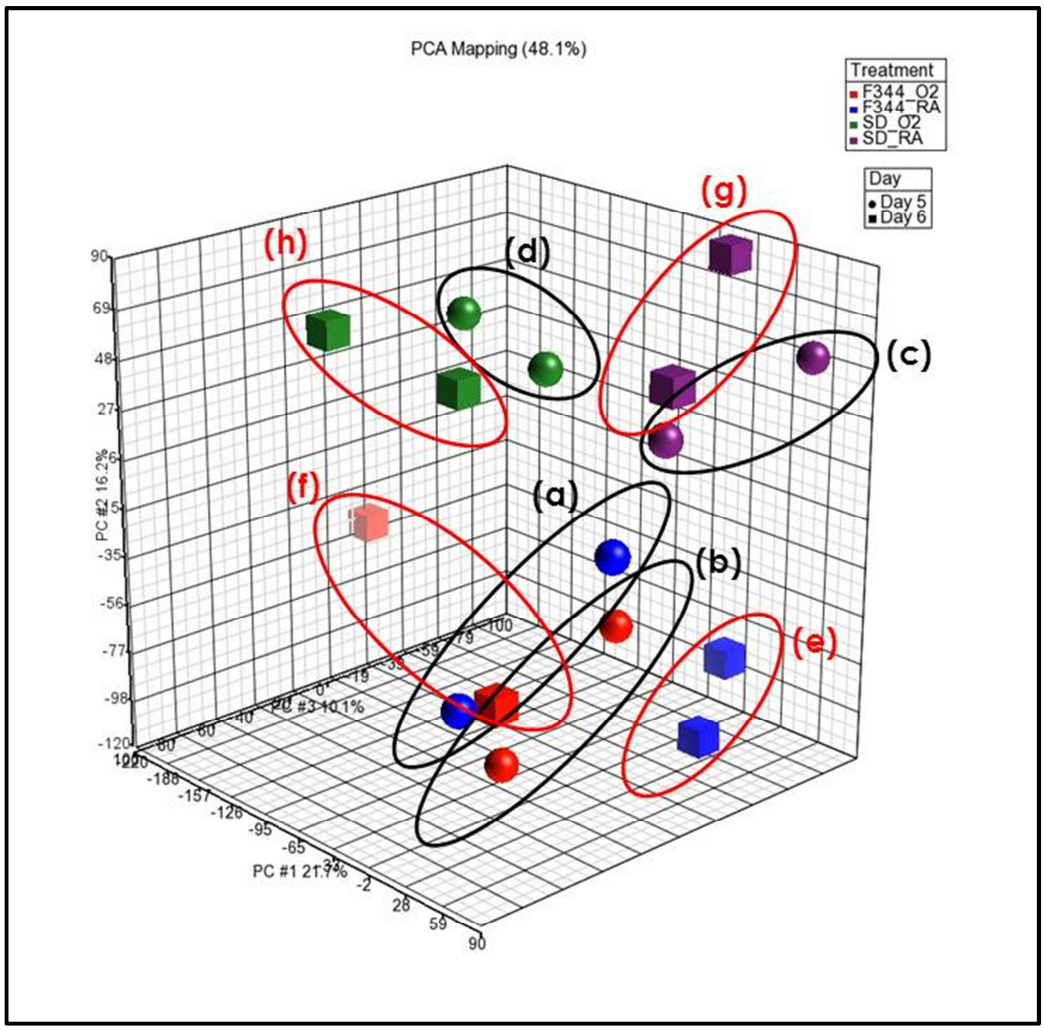

Figure 4.5 Principal component analysis of day 5 and 6 samples (n=2). (a) Day 5 F344 rats raised in room air, (b) Day 5 F344 rats exposed to cyclic hyperoxia from birth, (c) Day 5 SD rats raised in room air, (d) Day 5 SD rats exposed to cyclic hyperoxia from birth, (e) Day 6 F344 rats raised in room air, (f) Day 6 F344 rats exposed to cyclic hyperoxia from birth, (g) Day 6 SD rats raised in room air, (h) Day 6 SD rats exposed to cyclic hyperoxia from birth. Samples clustered according to strain and exposure to cyclic hyperoxia at both time points. Samples were considered to group in an acceptable manner to be included in the overall analysis of mRNA expression.

4.2.a.2 Number of genes which reached statistical significance

Correction for multiple comparisons yielded relatively few genes with significant adjusted p values at day 3; however, many more genes reached statistical significance at days 5 and 6 (Table 4.2).

Comparison	**Number of genes with significant adjusted p values**		
	DAY 3	**DAY 5**	**DAY 6**
FRA vs. SDRA	12	21	728
FO_2 vs. FRA	0	0	1
SDO_2 vs. SDRA	0	0	0
FO_2 vs. SDO_2	11	72	44

Table 4.2 Summary of significant adjusted p values at each time point. The number of genes with significant p values after using step-up correction for multiple comparisons for each time point and each comparison is shown. Significance level: 0.05; False Discovery Rate level 0.05; total number of p-values > 27,000 at each time point. FRA = F344 room air-exposed; SDRA = SD room air-exposed; FO_2 = F344 cyclic hyperoxia-exposed; SDO_2 = cyclic hyperoxia-exposed.

A majority of differentially expressed genes were as a result of strain differences in the FRA vs. SDRA comparison. The number of genes which reached statistical significance after adjustment for multiple comparisons, and were regulated by oxygen and strain (FO_2 vs. SDO_2 comparison) increased with increasing age of neonatal rats. There was overlap observed in the differentially expressed genes which reached statistical significance at

days 3, 5 and 6 in the FO_2 vs. SDO_2 comparison (Figure 4.6). A complete list of the genes differentially expressed in the FO_2 vs. SDO_2 comparison, including genes which were represented at a statistically significant level, is shown in Table 4.3. Selected genes with significant adjusted p values will be discussed in 4.2.b.1 and 4.2.b.2.

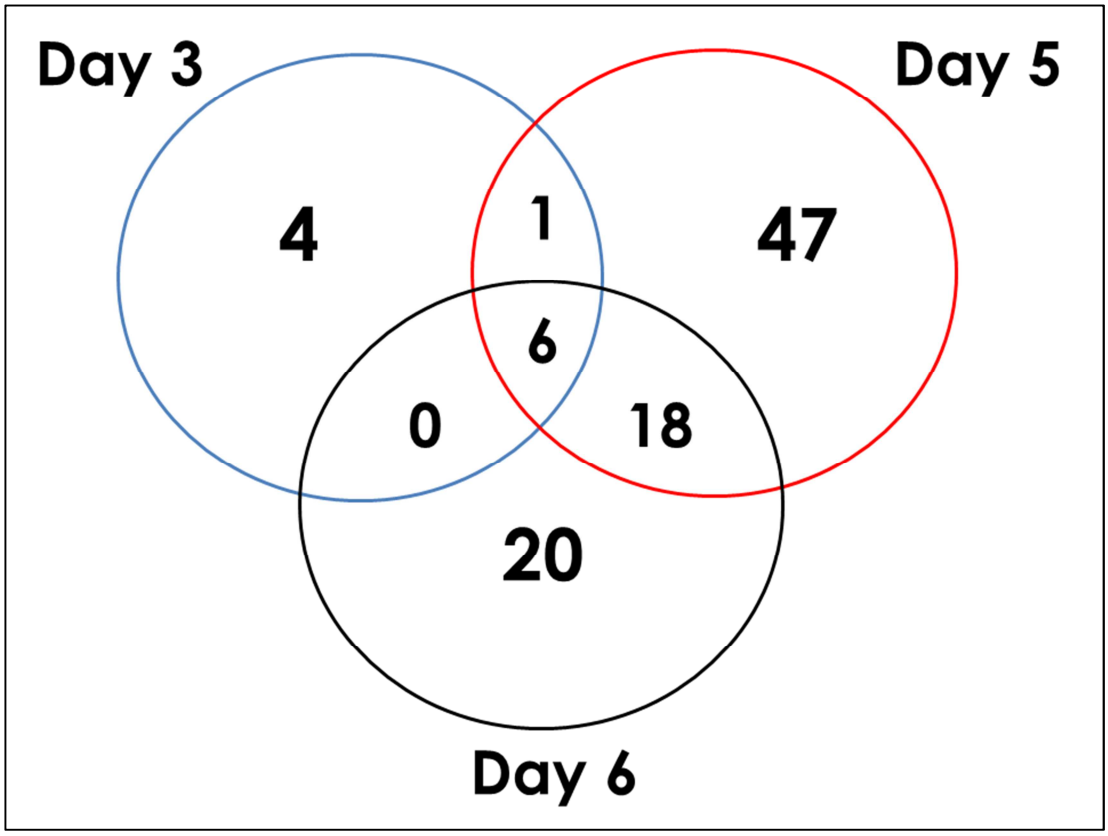

Figure 4.6 Venn diagram of genes with significant adjusted p values for the FO_2 vs. SDO_2 comparison at each time point. The number of genes which reach statistical significance at each time point is shown, along with genes which are represented at more than one time point.

Table 4.3 Genes which reached statistical significance at days 3, 5 and 6 in the FO_2 vs. SDO_2 comparison. Genes which reach statistical significance at a specific time point is shown, along with genes which are represented at more than one time point. Genes are shown in order of ascending p value; $p<0.05$. Unknown= gene which has not been identified but is included in the Affymetrix probeset.

Time point	Number of genes which reached statistical significance	Genes
Day 3	4	Hey2, RGD1564739, unknown, RGD1562660
Days 3 and 5	1	RGD156028
Days 3 and 6	0	-
Day 5	47	Dppa3, Olr1662, Glrx3, Rxrb, Ncr3, RGD1305311, Rbm41, RT1-Bb, RGD1561785, Akr1b1, RGD1307934, Bat5, Grm6, Znf692, Fth1, MGC72974, Snx26,Aga, Wdr81, Gabra5, Sgk493, RGD1564067, Ing2, Zfp347, Grm2, Cstf2t, Rbmxrtl, RGD1307325, Adcy6, St13, Ptgr1, Npas1
Days 5 and 6	18	Dnajc12, Otud6b, Cd9, Pter, H2-Ob, Car8, Ush1c, Alg8, LOC685105, Pax4, Ptn, Fancl, Gas8, Slu7, Chchd4, Nit2, Rab3b, Crb1
Day 6	20	Tmem176a, Cfh, LOC500584, Tmco3, Ly6g6d, Kdelr3, Zbtb37 and 13 unknown genes
Days 3, 5 and 6	6	Mospd1, Ly6g6e, Slc26a7, Tap2, Stk32a, Slc26a7

4.2.b Identification of candidate genes involved in susceptibility to OIR

A bioinformatics approach was used to investigate the large amount of gene expression data generated by the microarray screens and to place them in a biological context. An initial microarray screen was performed at day 3, followed by a second screen using samples from day 5 and separate samples from day 6. As a result, a total of 888 genes were found to be statistically significant in their differential expression in all the comparisons tested and at all time points. Analysis of genes which were differentially expressed in response to strain and treatment (FO_2 vs. SDO_2 comparison) still yielded 127 genes which were statistically significant. Genes that were differentially regulated by both strain and oxygen were of great interest, as they may provide insight into the basis of genetic susceptibility to OIR. Given that it was not possible to confirm the results of all 127 genes (at a minimum) using quantitative real-time RT-PCR, a filter was applied to select candidate genes that may be involved in the differential susceptibility to OIR. Therefore, genes that had significant adjusted p values ($p<0.05$), were regulated by oxygen, or oxygen and strain, or had previously been associated with OIR/ROP based on a search of the literature were investigated for confirmation of microarray results.

4.2.b.1 Identification of candidate genes at day 3

The entire Affymetrix microarray dataset for all comparisons performed at day 3 can be found in NCBI's Gene Expression Omnibus, and can be accessible through the GEO Series accession number GSE18998 (http://www.ncbi.nlm.nih.gov/geo/query/acc.cgi?acc=GSE18998). An electronic version of the datasets from days 3, 5 and 6 may be made available upon request.

Comparisons of gene expression between room air-exposed F344 and SD rats showed 11 genes to be significantly regulated by strain at day 3 (Table 4.4). A comparison of cyclic hyperoxia-exposed F344 and SD rats showed that ten genes were differentially expressed to a significant level (Table 4.5). The majority of these genes were represented in the F344 room air-exposed vs. SD room air-exposed comparison, and so were not of particular interest.

No significant changes in gene expression were seen in F344 rats exposed to cyclic hyperoxia for 3 days compared to room air-exposed rats. Similarly, no significant changes were observed in cyclic-hyperoxia exposed SD rats compared with room air-exposed controls. In both comparisons, adjusted p values were greater than 0.05.

Table 4.4 Genes significantly regulated by strain in RA-exposed F344 and SD rats at day 3. Adjusted p value < 0.05; +/- indicates over- or under-expression of the gene, respectively. [a] Gene is represented by a second exon in the array with a fold change of 17.45 and an adjusted p value of 0.015; [b] Affymetrix probeset ID of a gene which has not been identified.

Gene	*Gene Description*	*Fold Change*	*Fold Change Description at Day 3*	*Adjusted p Value*
Mospd1[a]	Motile sperm domain containing 1	22.43	FRA up vs. SDRA	0.015
RGD1564739	Akin to spermatogenesis associated glutamate (E)-r	-3.98	FRA down vs. SDRA	0.015
Slc26a7	Solute carrier family 26, member 7	-4.10	FRA down vs. SDRA	0.022
Ly6g6e	Lymphocyte antigen 6 complex, locus G6E	3.25	FRA up vs. SDRA	0.026
Tap2	Transporter 2, ATP-binding cassette, sub-family B	5.56	FRA up vs. SDRA	0.029
Hey2	Hairy/enhancer-of-split related with YRPW motif 2	1.23	FRA up vs. SDRA	0.035
10722435[b]	Unknown	-20.69	FRA down vs. SDRA	0.035
Stk32a	Serine/threonine kinase 32A	-4.99	FRA down vs. SDRA	0.041
Oprk1	Opioid receptor, kappa 1	2.34	FRA up vs. SDRA	0.041
Arsb	Arylsulfatase B	-2.66	FRA down vs. SDRA	0.048
RGD1310110	Similar to 3632451O06 Rik protein	-1.44	FRA down vs. SDRA	0.048

Table 4.5 Genes significantly regulated by strain in cyclic hyperoxia-exposed F344 and SD rats at day 3. Adjusted p value < 0.05; +/- indicates over- or under-expression of the gene, respectively. [a] Gene is represented by a second exon in the array with a fold change of 17.46 and an adjusted p value of 0.01; [b] Affymetrix probeset ID of a gene which has not been identified

Gene	*Gene Description*	*Fold Change*	*Fold Change Description at Day 3*	**Adjusted p Value**
Mospd1[a]	Motile sperm domain containing 1	21.80	F344 O_2 up vs. SD O_2	0.012
Ly6g6e	Lymphocyte antigen 6 complex, locus G6E	4.55	F344 O_2 up vs. SD O_2	0.012
Slc26a7	Solute carrier family 26, member 7	-4.77	F344 O_2 down vs. SD O_2	0.012
Hey2	Hairy/enhancer-of-split related with YRPW motif 2	1.32	F344 O_2 up vs. SD O_2	0.012
RGD1564739	Akin to spermatogenesis associated glutamate (E)-r	-3.30	F344 O_2 down vs. SD O_2	0.016
Tap2	Transporter 2, ATP-binding cassette, sub-family B	5.64	F344 O_2 up vs. SD O_2	0.024
10722435[b]	Unknown	-18.64	F344 O_2 down vs. SD O_2	0.033
Stk32a	Serine/threonine kinase 32A	-5.69	F344 O_2 down vs. SD O_2	0.033
RGD1562660	RGD1562660	-1.33	F344 O_2 down vs. SD O_2	0.033
RGD1560289	Similar to chromosome 3 open reading frame 20	-2.50	F344 O_2 down vs. SD O_2	0.042

4.2.b.1.a Fold change analysis of differentially regulated genes at day 3

In each of the 4 comparisons, the number of genes that showed a change of at least ± 1.5 fold accounted for 1.0% or less of the total number of genes represented on the microarrays. Whilst 1.5 fold changes in gene expression may appear modest, several microarray studies using clinical samples derived from human liver samples have found that a 1.5 fold change is sufficient to have a biologically relevant effect [228-230].

Because no hyperoxia-regulated genes reached statistical significance following correction for multiple comparisons in the initial analyses, an alternative approach was required. Lists of genes which were differentially expressed in response to cyclic hyperoxia were submitted to the freely available online database, Database for Annotation, Visualisation and Integrated Discovery (DAVID; http://david.abcc.ncifcrf.gov/) [231, 232]. DAVID was used to analyse gene lists derived from high-throughput genomic experiments. Pathways showing enrichment for specific genes were found using the functional annotation and chart pathway-mining tools.

For each strain, genes that differed between cyclic hyperoxia and room air-exposed groups were ranked by fold change. The top fifty upregulated and downregulated genes were submitted to DAVID, to identify enriched gene groups (Table 4.6). Initial DAVID analysis at day 3 using fold changes to rank differentially expressed genes was performed by Rhys Fogarty (Department

of Ophthalmology, Flinders University, SA, Australia). All other analyses were performed by myself.

Genes from both strains were enriched for Gene Ontology (GO) terms related to carbohydrate metabolism. More of these terms appeared in the SD list compared to the F344 list. The SD list showed strong enrichment for genes involved in glycolysis, a process known to be affected by oxygen levels. In addition, the SD list returned the GO term 'Response to Hypoxia' which was absent from the F344 list. Manual analysis of the gene lists showed that many genes known to be upregulated by HIF-1α in response to hypoxia were downregulated in response to hyperoxia at day 3 (Table 4.7).

Table 4.6 DAVID analysis for Gene Ontology terms enriched in the top fifty genes (ranked by fold change) that were upregulated or downregulated by cyclic hyperoxia in each strain at day 3. GO terms are ranked by fold enrichment. A) Fold enrichment – The ratio between the frequency of term-annotated genes in the query gene list compared to the reference gene list, in this case the rat genome. B) False discovery rate – the expected percentage of false positives in a given proportion of genes considered to be significant

GO TERM	**NUMBER OF GENES**	**Fold enrichment [a]**	**False Discovery Rate [b]**
F344			
Cellular carbohydrate catabolic process	8	9.6	0.033
Carbohydrate catabolic process	8	9.1	0.049
SD			
Glycolysis	8	18.6	3.72E-04
Glucose catabolic process	8	15.9	0.001
Response to hypoxia	8	15.6	0.001
Hexose catabolic process	8	15.2	0.001
Monosaccharide catabolic process	8	15.2	0.001
Alcohol catabolic process	8	14.7	0.001
Cellular carbohydrate catabolic process	8	11.8	0.008
Glucose metabolic process	9	11.4	0.002
Carbohydrate catabolic process	8	11.1	0.012
Monosaccharide metabolic process	11	11.0	8.62E-05
Hexose metabolic process	10	10.1	9.22E-04
Soluble fraction	9	7.3	0.038
Alcohol metabolic process	12	7.1	0.001
Cellular carbohydrate metabolic process	12	6.9	0.002
Carbohydrate metabolic process	13	5.3	0.007

Table 4.7 Known hypoxia-regulated genes identified from the top fifty genes (ranked by fold change) that were downregulated by cyclic hyperoxia in each strain compared to room air exposure at day 3. Only genes with a fold change of greater than ± 1.5 fold are shown.

Gene	Gene Description	Fold Change
Genes downregulated by hyperoxia in F344 rats		
Adra1b	Adrenergic, alpha-1B-, receptor	-2.12
Igfbp2	Insulin-like growth factor binding protein 2	-1.86
Slc16a3	Solute carrier family 16, member 3	-1.86
Cox4i2	Cytochrome c oxidase subunit IV isoform 2	-1.58
Genes downregulated by hyperoxia in SD rats (continued next page)		
Slc16a3	Solute carrier family 16, member 3	-4.10
Igfbp2	Insulin-like growth factor binding protein 2	-3.42
Hk2	Hexokinase 2	-2.95
Pfkfb3	6-phosphofructo-2-kinase/fructose-2,6-biphosphatase 3	-2.80
Egln3	EGL nine homolog 3	-2.79
Bnip3	BCL2/adenovirus E1B 19 kDa-interacting protein 3	-2.63
Cox4i2	Cytochrome c oxidase subunit IV isoform 2	-2.45
Pdk1	Phosphoglycerate kinase 1	-2.31
Vegf A	Vascular endothelial growth factor A	-2.23
P4ha1	Procollagen-proline, 2-oxoglutarate 4-dioxygenase	-2.20
Mif	Macrophage migration inhibitory factor	-2.01
Ak3l1	Adenylate kinase 3-like 1	-1.97
Pfkl	Phosphofructokinase, liver	-1.93
Tpi1	Triosephosphate isomerase 1	-1.89
Egln1	EGL nine homolog 1	-1.72

Genes downregulated by hyperoxia in SD rats (continued from previous page)		
Gene	**Gene Description**	**Fold Change**
Bhlhb2	Basic helix-loop-helix family, member e40	-1.67
Ldha	Lactate dehydrogenase A	-1.62
Pgk1	Phosphoglycerate kinase 1	-1.61
Aldoa	Aldolase A, fructose-bisphosphate	-1.57
Gpi	Glucose phosphate isomerase	-1.56

4.2.b.2 Identification of candidate genes at days 5 and 6

As there were many more genes which had significant adjusted p values ($p<0.05$) after correction for multiple comparisons at day 5 and 6 compared to day 3, a modified approach was used to identify candidate genes.

4.2.b.2.a Identification of candidate genes at day 5

At day 5, 78 genes with significant adjusted p values from the FO_2 vs. SDO_2 comparison were cross-referenced against 21 genes which were statistically significant in the FRA vs. SDRA comparison, to identify genes that were unique to either list. Fifty seven such genes were identified, 7 of which were unknown genes. As a result, 50 genes were submitted to DAVID for functional annotation as shown in Table 4.8. Functional annotation of the gene list showed enrichment for GO terms related to synaptic transmission and behaviour as shown in Table 4.9.

Table 4.8 Differentially expressed unique gene candidates at day 5 ranked by adjusted p value and comparison. Gene lists from the FO_2 vs. SDO_2 comparison were cross-referenced against the FRA vs. SDRA comparison. A total of 50 potential gene candidates were identified using this method. Genes shown in red are genes which were differentially expressed in the FRA vs. SDRA comparison. Genes shown in black were differentially expressed in the FO_2 vs. SDO_2 comparison. + Gene candidate Dppa3 is represented more than once in the gene list as multiple exons are used in the array.

Gene	*Gene Description*	*Fold Change*	*Fold Change Description at Day 5*	*Adjusted p Value*
LOC500705	Similar to chromosome 14 open reading frame 143	1.79984	FRA up vs. SDRA	0.0470000
Oprk1	Opioid receptor, kappa 1	2.14331	FRA up vs. SDRA	0.0470000
Dnajc12	DnaJ (Hsp40) homolog, subfamily C, member 12	-1.48478	FO2 down vs. SDO2	0.00633494
Dppa3 +	Developmental pluripotency-associated 3	-1.7193	FO2 down vs. SDO2	0.00782835
Olr1662	Olfactory receptor 1662	-1.26986	FO2 down vs. SDO2	0.00900528
Dppa3	Developmental pluripotency-associated 3	-1.6836	FO2 down vs. SDO2	0.00900528
Alg8	Asparagine-linked glycosylation 8, alpha-1,3-glucosyltransferase family	-1.61751	FO2 down vs. SDO2	0.0105507
Ush1c	Usher syndrome 1C homolog (human)	-1.47154	FO2 down vs. SDO2	0.0105507
Car8	NCarbonic anhydrase 8	-1.76489	FO2 down vs. SDO2	0.0105507
Glrx3	Glutaredoxin 3	1.66503	FO2 up vs. SDO2	0.0168103
Ptn	Pleiotrophin	-1.75756	FO2 down vs. SDO2	0.0171373
Fancl	Fanconi anaemia, complementation group L	-1.64305	FO2 down vs. SDO2	0.0171373
Gas8	Growth arrest specific 8	-1.56467	FO2 down vs. SDO2	0.0190486
Rxrb	Retinoid X receptor beta	1.49173	FO2 up vs. SDO2	0.0206839
Ncr3	Natural cytotoxicity triggering receptor 3	-1.13868	FO2 down vs. SDO2	0.0215687

Gene	*Gene Description*	*Fold Change*	*Fold Change Description at Day 5*	*Adjusted p Value*
Slu7	SLU7 splicing factor homolog (*S. cerevisiae*)	-1.48	FO2 down vs. SDO2	0.0215687
RGD1305311	Similar to hypothetical protein FLJ22527	-1.36142	FO2 down vs. SDO2	0.0227706
Rbm41	RNA binding motif protein 41	-2.11685	FO2 down vs. SDO2	0.0281037
Chchd4	Coiled-coil-helix-coiled-coil-helix domain containing 4	-1.65848	FO2 down vs. SDO2	0.0306076
RGD1561785	Similar to mKIAA1924 protein	1.51971	FO2 up vs. SDO2	0.0306076
RT1-Bb	RT1 class II, locus Bb	-3.43213	FO2 down vs. SDO2	0.0306076
Akr1b1	Aldo-keto reductase family 1, member B1 (aldose reductase)	1.77246	FO2 up vs. SDO2	0.0320907
Grm6	Glutamate receptor, metabotropic 6	2.1931	FO2 up vs. SDO2	0.0345702
Rab3b	RAB3B, member RAS oncogene family	-1.98831	FO2 down vs. SDO2	0.0345702
Dppa3	Developmental pluripotency-associated 3	-1.64661	FO2 down vs. SDO2	0.0345702
RGD1307934	Similar to DNA segment, Chr 19, ERATO Doi 38	-1.51658	FO2 down vs. SDO2	0.0345702
Bat5	HLA-B associated transcript 5	1.89264	FO2 up vs. SDO2	0.0345702
Nit2	Nitrilase family, member 2	-2.19853	FO2 down vs. SDO2	0.0345702
Znf692	Zinc finger protein 692	-1.47276	FO2 down vs. SDO2	0.0355043
RGD1561785	Similar to mKIAA1924 protein	1.38346	FO2 up vs. SDO2	0.0357678
Fth1	Ferritin, heavy polypeptide 1	2.75538	FO2 up vs. SDO2	0.0367704
RGD1560289	Similar to chromosome 3 open reading frame 20	-2.14211	FO2 down vs. SDO2	0.0367704
Snx26	Sorting nexin 26	1.6167	FO2 up vs. SDO2	0.0377961
MGC72974	Hypothetical LOC316976	-2.7658	FO2 down vs. SDO2	0.0377961

Gene	***Gene Description***	***Fold Change***	***Fold Change Description at Day 5***	***Adjusted p Value***
Aga	Aspartylglucosaminidase	-1.20753	FO2 down vs. SDO2	0.0400907
RGD1561785	Similar to mKIAA1924 protein	2.12866	FO2 up vs. SDO2	0.0400907
Gabra5	Gamma-aminobutyric acid (GABA) A receptor, alpha 5	1.31602	FO2 up vs. SDO2	0.042392
RGD1561785	Similar to mKIAA1924 protein	1.78496	FO2 up vs. SDO2	0.042392
Crb1	Crumbs homolog 1 (Drosophila)	-1.55634	FO2 down vs. SDO2	0.042392
Wdr81	WD repeat domain 81	1.34111	FO2 up vs. SDO2	0.042392
Sgk493	Protein kinase-like protein SgK493	1.42952	FO2 up vs. SDO2	0.0430391
RGD1564067	Similar to RIKEN cDNA 1700022C21	-2.99919	FO2 down vs. SDO2	0.0434626
Ing2	Inhibitor of growth family, member 2	-1.46288	FO2 down vs. SDO2	0.043904
Zfp347	Zinc finger protein 347	-1.21417	FO2 down vs. SDO2	0.0439262
Grm2	Glutamate receptor, metabotropic 2	1.95121	FO2 up vs. SDO2	0.0453729
Cstf2t	Cleavage stimulation factor, 3' pre-RNA subunit 2, tau variant	-1.64309	FO2 down vs. SDO2	0.0462408
Rbmxrtl	RNA binding motif protein, X chromosome retrogene-like (*Rattus norvegicus)*	-1.45314	FO2 down vs. SDO2	0.0462408
RGD1307325	Similar to RIKEN cDNA 4933411K20	-1.39838	FO2 down vs. SDO2	0.0474105
Adcy6	Adenylate cyclase 6	1.4211	FO2 up vs. SDO2	0.0485848
St13	Suppression of tumorigenicity 13	-1.25658	FO2 down vs. SDO2	0.0487207
Npas1	Neuronal PAS domain protein 1	1.17431	FO2 up vs. SDO2	0.0488326
Ptgr1	Prostaglandin reductase 1	-1.87806	FO2 down vs. SDO2	0.0488326

GO Term	Number of genes	Fold enrichment [a]	False Discovery Rate [b]
Synaptic transmission	4	7.6	17.015
Behaviour	5	4.9	19.158

Table 4.9 DAVID analysis for Gene Ontology terms enriched in the 57 unique genes with significant adjusted p values yielded from cross-referencing the FO2 vs. SDO2 and FRA vs. SDRA comparisons. GO terms are ranked by fold enrichment. A) Fold enrichment – The ratio between the frequency of term-annotated genes in the query gene list compared to the reference gene list, in this case the rat genome. B) False discovery rate – the expected percentage of false positives in a given proportion of genes considered to be significant

4.2.b.2.b Identification of candidate genes at day 6

At day 6, 45 genes with significant adjusted p values from the FO_2 vs. SDO_2 comparison were cross-referenced against the top 100 genes of the 628 genes with significant adjusted p values from the FRA vs. SDRA comparison. The top 100 genes from the FRA vs. SDRA comparison were chosen to limit the number of unique candidates identified that were differentially expressed as a result of strain differences. Cross-referencing the two gene lists resulted in the identification of 70 unique genes, 10 of which were unknown genes. An additional 2 genes from the FO_2 vs. FRA comparison were also added to the candidate gene list. One gene had a significant adjusted p value and the other gene was borderline significant after correction for multiple comparisons. A total of 72 genes were submitted for functional annotation using DAVID. The gene list is shown in Table 4.10.

Table 4.10 Differentially expressed unique gene candidates at day 6 ranked by adjusted p value and comparison. Gene lists from the FO_2 vs. SDO_2 comparison were cross-referenced against the FRA vs. SDRA comparison. A total of 72 gene candidates were identified. Genes shown in orange are genes which were differentially expressed in the FO_2 vs. FRA comparison. Genes shown in green were differentially expressed in the FO_2 vs. SDO_2 comparison. Genes shown in black were differentially expressed in the FRA vs. SDRA comparison. + Gene candidate Crat is represented more than once in the gene list as multiple exons are used in the array and was significant in two different comparisons. # Gene candidate Pdcl is represented more than once in the gene list as multiple exons are used in the array.

Gene	*Gene Description*	*Fold Change*	*Fold Change Description at Day 6*	*Adjusted p Value*
Crat +	Carnitine acetyltransferase	-1.52006	FO2 down vs. FRA	0.0192131
Aga	Aspartylglucosaminidase	1.38236	FO2 up vs. FRA	0.0518171
Ush1c	Usher syndrome 1C homolog (human)	-1.53117	FO2 down vs. SDO2	0.0192511
Car8	Carbonic anhydrase 8	-1.77255	FO2 down vs. SDO2	0.0240441
Tmem176a	Transmembrane protein 176A	-2.21607	FO2 down vs. SDO2	0.0256494
LOC500584	Similar to casein kinase 1, gamma 3 isoform 2	-1.55212	FO2 down vs. SDO2	0.032945
Tmco3	Transmembrane and coiled-coil domains 3	-3.0724	FO2 down vs. SDO2	0.0476045
Ly6g6d	Lymphocyte antigen 6 complex, locus G6D	3.81517	FO2 up vs. SDO2	0.0476045
Rab3b	RAB3B, member RAS oncogene family	-1.9514	FO2 down vs. SDO2	0.0476045
Kdelr3	KDEL (Lys-Asp-Glu-Leu) endoplasmic reticulum protein retention receptor 3	-1.52302	FO2 down vs. SDO2	0.0476045
Zbtb37	Zinc finger and BTB domain containing 37	1.3987	FO2 up vs. SDO2	0.0476045

Gene	*Gene Description*	*Fold Change*	*Fold Change Description at Day 6*	*Adjusted p Value*
Zfp347	Zinc finger protein 347	-1.66731	FRA down vs. SDRA	0.00209438
Crat	Carnitine acetyltransferase	1.49564	FRA up vs. SDRA	0.00312812
Sgk493	Protein kinase-like protein SgK493	2.01415	FRA up vs. SDRA	0.0040332
RGD1561785	Similar to mKIAA1924 protein	1.78964	FRA up vs. SDRA	0.00418981
RGD1307934	Similar to DNA segment, Chr 19, ERATO Doi 38	-1.96367	FRA down vs. SDRA	0.00511382
Rxrb	Retinoid X receptor beta	1.65928	FRA up vs. SDRA	0.00736852
St13	Suppression of tumorigenicity 13	-1.46961	FRA down vs. SDRA	0.00769535
RGD1561785	Similar to mKIAA1924 protein	1.71485	FRA up vs. SDRA	0.0101085
Slc22a17	Solute carrier family 22, member 17	1.92716	FRA up vs. SDRA	0.0101085
Grm2	Glutamate receptor, metabotropic 2	2.68622	FRA up vs. SDRA	0.0107047
Akr1b1	Aldo-keto reductase family 1, member B1 (aldose reductase)	1.96008	FRA up vs. SDRA	0.0112663
Abca8a	ATP-binding cassette, sub-family A (ABC1), member 8a	-1.37375	FRA down vs. SDRA	0.0112663
Bat5	HLA-B associated transcript 5	2.30504	FRA up vs. SDRA	0.0112663
Dexi	Dexamethasone-induced transcript	1.45093	FRA up vs. SDRA	0.0112663
Adcy6	Adenylate cyclase 6	1.6747	FRA up vs. SDRA	0.0112663
Wdr81	WD repeat domain 81	1.49759	FRA up vs. SDRA	0.0112663

Gene	*Gene Description*	*Fold Change*	*Fold Change Description at Day 6*	*Adjusted p Value*
Zbtb17	Zinc finger and BTB domain containing 17	1.40496	FRA up vs. SDRA	0.0112663
Fam110a	Family with sequence similarity 110, member A	1.72333	FRA up vs. SDRA	0.0112663
Loxl1	Lysyl oxidase-like 1	3.44432	FRA up vs. SDRA	0.0112663
St13	Suppression of tumorigenicity 13	-1.51437	FRA down vs. SDRA	0.0112663
LOC310926	Hypothetical protein LOC310926	1.77334	FRA up vs. SDRA	0.0112663
Ncr3	Natural cytotoxicity triggering receptor 3	-1.14698	FRA down vs. SDRA	0.0112663
St13	Suppression of tumorigenicity 13	-1.49192	FRA down vs. SDRA	0.0112663
Snx26	Sorting nexin 26	1.82624	FRA up vs. SDRA	0.0112663
Grn	Granulin	1.44387	FRA up vs. SDRA	0.0112663
Pdcl #	Phosducin-like	-1.40201	FRA down vs. SDRA	0.0112663
Fibp	Fibroblast growth factor (acidic) intracellular binding protein	2.28159	FRA up vs. SDRA	0.0112663
P76	Mannose-6-phosphate protein p76	2.19269	FRA up vs. SDRA	0.0112663
Btbd2	BTB (POZ) domain containing 2	2.10905	FRA up vs. SDRA	0.0112663
Nnat	Neuronatin	1.68576	FRA up vs. SDRA	0.0112663
Ptov1	Prostate tumour overexpressed 1	2.63609	FRA up vs. SDRA	0.0114976
Mtvr2	Mammary tumour virus receptor 2	2.49971	FRA up vs. SDRA	0.0115739

Gene	*Gene Description*	*Fold Change*	*Fold Change Description at Day 6*	*Adjusted p Value*
Xrcc1	X-ray repair complementing defective repair in Chinese hamster cells 1	1.43045	FRA up vs. SDRA	0.0115739
Rbm41	RNA binding motif protein 41	-2.19516	FRA down vs. SDRA	0.0118527
St7l	Suppression of tumorigenicity 7-like	-1.62614	FRA down vs. SDRA	0.0124472
Neurl4	Neutralised homolog 4 (Drosophila)	1.4939	FRA up vs. SDRA	0.012581
Ptdss2	Phosphatidylserine synthase 2	1.43779	FRA up vs. SDRA	0.0135479
Ing2	Inhibitor of growth family, member 2	-1.58482	FRA down vs. SDRA	0.0141479
Timm23	Translocase of inner mitochondrial membrane 23 homolog (yeast)	1.55377	FRA up vs. SDRA	0.0143898
Rap1gap	Rap1 GTPase-activating protein	3.0459	FRA up vs. SDRA	0.0143898
Ptgr1	Prostaglandin reductase 1'	-2.19749	FRA down vs. SDRA	0.0143898
Fgf9	Fibroblast growth factor 9	-1.46717	FRA down vs. SDRA	0.0143898
Pdcl	Phosducin-like	-1.55503	FRA down vs. SDRA	0.0143898
Msl1	Male-specific lethal 1 homolog (Drosophila)	1.50528	FRA up vs. SDRA	0.0143898
Pir	Pirin (iron-binding nuclear protein)	-2.05165	FRA down vs. SDRA	0.0143898
Fxyd6	FXYD domain-containing ion transport regulator 6	1.93737	FRA up vs. SDRA	0.0143898
Th	Tyrosine hydroxylase	1.68977	FRA up vs. SDRA	0.0143898
Dvl1	Dishevelled, dsh homolog 1 (Drosophila)	2.14063	FRA up vs. SDRA	0.0143898

Gene	*Gene Description*	*Fold Change*	*Fold Change Description at Day 6*	*Adjusted p Value*
RGD1305455	Similar to hypothetical protein FLJ10925	1.58332	FRA up vs. SDRA	0.0143898
Ubxn6	UBX domain protein 6	1.40366	FRA up vs. SDRA	0.0143898
Pgbd5	PiggyBac transposable element derived 5	1.34596	FRA up vs. SDRA	0.0143898
Ecel1	Endothelin converting enzyme-like 1	1.61142	FRA up vs. SDRA	0.0143898
Dpysl4	Dihydropyrimidinase-like 4	1.66321	FRA up vs. SDRA	0.0143898
Trim28	Tripartite motif-containing 28	1.44791	FRA up vs. SDRA	0.0143898
Eif2c1	Eukaryotic translation initiation factor 2C, 1	1.448	FRA up vs. SDRA	0.0143898
Ecat1	ES cell associated transcript 1	-1.24694	FRA down vs. SDRA	0.0151691
Mrps14	Mitochondrial ribosomal protein S14	-1.6823	FRA down vs. SDRA	0.0151691
Agrn	Agrin	1.55945	FRA up vs. SDRA	0.0155611
LOC365723	Similar to zinc finger protein 458	-1.63359	FRA down vs. SDRA	0.0156451
RGD1307325	Similar to RIKEN cDNA	-1.46948	FRA down vs. SDRA	0.0161003
LOC680073	Similar to globin inducing factor, foetal	-1.50105	FRA down vs. SDRA	0.0161373
RGD1561785	Similar to mKIAA1924 protein	2.25331	FRA up vs. SDRA	0.0161373

Functional annotation of the gene list showed enrichment for GO terms related to cell-cell signalling, synaptic transmission and transition metal ion binding as shown in Table 4.11

GO term	Number of genes	Fold enrichment a	False Discovery Rate b
Synaptic transmission	5	7.7	3.4489
Cell – cell signalling	6	6.1	3.4489
Transition metal ion binding	12	2.2	13.2480

Table 4.11 DAVID analysis for Gene Ontology terms enriched in the 72 unique genes with significant adjusted p values yielded from cross-referencing the FO_2 vs. SDO_2 and FRA vs. SDRA comparisons and from the FO_2 vs. FRA comparison. GO terms are ranked by fold enrichment. A) Fold enrichment – The ratio between the frequency of term-annotated genes in the query gene list compared to the reference gene list, in this case the rat genome. B) False discovery rate – the expected percentage of false positives in a given proportion of genes considered to be significant.

4.2.c Selection of gene candidates for validation at days 3, 5 and 6.

A final filter was applied to select genes of interest. Genes for confirmation of microarray results using quantitative real-time RT-PCR were chosen if they were shown to be regulated by oxygen with a minimum 1.5 fold change in expression in response to cyclic hyperoxia exposure. Based on functional annotation of differentially expressed genes at days 3 using DAVID (Table 4.6), 7 genes were chosen for confirmation of microarray results: EGLN3,

EGLN1, SLC16A3, HK2, BNIP3, IGFBP2 and IGFBP3. IGFBP3 had previously een associated with OIR/ROP based on a search of the literature.

Functional annotation of genes that were differentially expressed at days 5 (Table 4.9) and 6 (Table 4.11) showed these genes were related to neurological cell-cell signalling and metal ion binding. The relevance of these genes to susceptibility to OIR is unclear; therefore they were not investigated further.

Despite the fact there were other genes which also showed regulation by cyclic hyperoxia at day 3 as shown in Table 4.7, they did not appear to be directly relevant to OIR, therefore they were not given priority for confirmation of microarray results. The 7 genes chosen for confirmation did show relevance to OIR and will be discussed in turn.

4.2.c.1.a Prolyl hydroxylases EGLN3 and EGLN1

Results from the Affymetrix microarrays showed EGL nine homolog 3 (EGLN3, also known as PHD3) was downregulated 2.8 fold in SD rats in response to hyperoxia at day 3 remained but unchanged in F344 rats. At day 5, EGLN3 was downregulated in response to hyperoxia in F344 and SD rats 2.9 fold and 2.3 fold, respectively. In response to relative hypoxia at day 6, EGLN3 was unchanged in F344 rats and upregulated 1.9 fold in SD rats.

Expression of EGL nine homolog 1 (EGLN1, also known as PHD2) was downregulated 1.7 fold in SD rats in response to hyperoxia at day 3 but expression was unchanged in F344 rats. At day 5, EGLN1 was largely unchanged in both strains in response to hyperoxia. In response to relative hypoxia at day 6, EGLN1 was up-regulated 1.7 fold in SD rats, whereas expression was unchanged in F344 rats.

These data suggest there may be a strain-related difference in gene expression in response to cyclic hyperoxia in these two rat strains which differ in their susceptibility to OIR. EGLN3/PHD3 and EGLN1/PHD2 belong to a class of oxygen-dependent prolyl hydroxylases known to be involved in the regulation of a family of hypoxia-inducible factors (HIFs) in normoxia [233], and showed a strain-related difference in expression. Therefore these two genes were chosen for validation using quantitative real-time RT-PCR.

4.2.c.1.b Monocarboxylate transporter SLC16A3

Results from the Affymetrix microarrays showed the monocarboxylate transporter, solute carrier family 16 member 3 (SLC16A3), was downregulated 4.1 fold in SD rats in response to hyperoxia at day 3, and to a lesser extent in F344 rats with a 1.9 fold downregulation observed. At day 5, SLC16A3 was downregulated by hyperoxia in both strains, showing a fold change of 2.7 and 3.0 in F344 and SD rats respectively. Expression at day 6 in

response to relative hypoxia showed upregulation in both strains, with a 1.2 fold increase observed in F344 rats and a 1.7 fold increase in SD rats.

4.2.c.1.c BCL2/adenovirus interacting protein BNIP3

Affymetrix microarray showed BCL2/adenovirus E1B 19 kDa-interacting protein 3 (BNIP3), known to be involved in apoptotic processes [234], was downregulated 1.3 fold in F344 rats at day 3 in response to hyperoxia and 2.6 fold in SD rats. At day 5, BNIP3 expression was downregulated 1.9 and 1.8 fold respectively in F344 and SD rats. At day 6, BNIP3 was upregulated in both strains 1.3 fold.

4.2.c.1.d Glucose phosphorylation enzyme HK2

Expression of hexokinase 2 (HK2), a gene involved in glycolysis [235] was found to be unchanged in response to hyperoxia at day 3 in F344 rats, but downregulated 3.0 fold in SD rats. At day 5, expression was downregulated in both strains, with a 2.8 fold change observed in F344 rats, and a 2.5 fold change observed in SD rats. Expression at day 6 in response to relative hypoxia showed a similar upregulation in both strains, with a 1.4 and 1.3 fold change in F344 and SD rats, respectively.

4.2.c.1.e Insulin-like growth factor binding proteins IGFBP2 and IGFBP3

Expression of insulin-like growth factor binding protein 2 (IGFBP2) was downregulated by hyperoxia at days 3 and 5 in both strains. IGFBP2 was

downregulated 1.9 fold in F344 rats at day 3, 3.4 fold in SD rats also at day 3, and at day 5, IGFBP2 was downregulated 1.9 fold in both strains. At day 6, in response to relative hypoxia, IGFBP2 was upregulated 1.2 fold in F344 rats and 1.8 fold in SD rats.

Analysis of the literature showed expression of another member of the insulin-like growth factor binding protein family, IGFBP3, was protective against oxygen-induced vaso-obliteration in a mouse model of OIR [236]. Analysis of the Affymetrix microarrays showed IGFBP3 was slightly downregulated in response to cyclic hyperoxia in both strains at days 3 and 5 (<1.2 fold change in both strains). At day 6, IGFBP3 expression remained unchanged in response to relative hypoxia in both strains. Whilst IGFBP3 was not regulated by strain or cyclic hyperoxia exposure in this model of OIR, nonetheless it was chosen as another gene candidate for validation, given its importance in the mouse model of OIR.

4.3 STRAIN DIFFERENCES IN RETINAL GENE EXPRESSION FOLLOWING EXPOSURE TO CYCLIC HYPEROXIA

Expression of all 7 candidate genes was examined in room air and cyclic hyperoxia-exposed rats using quantitative real-time RT-PCR at day 3 to confirm microarray results using the same pooled RNA samples that were submitted for microarray analysis. Subsequent analysis of gene expression was performed EGLN3, ELGN1 and IGFBP3 at days 3, 5 and 6, using RNA

samples from individual rats to determine the of effect intra-strain variation. The collective results of these experiments are summarised in section 4.3.d.

4.3.a Confirmation of PCR primer specificity and determination of primer PCR amplification efficiencies

Primer specificity and determination of primer PCR amplification efficiencies were performed as described in section 2.4.l. Representative real-time RT-PCR fluorescence amplification plots and melt curves for EGLN3, EGLN1 and IGFBP3 are shown in section 4.3.a.1. Primer PCR amplification efficiencies for all 7 candidate genes are shown in section 4.3.a.2.

4.3.a.1 Confirmation of PCR primer specificity

All primer pairs for the 7 candidate genes chosen for confirmation by quantitative real-time RT-PCR were confirmed to be specific for the gene of interest and amplified a single PCR product, as confirmed by agarose gel electrophoresis and subsequent sequencing of purified PCR product, as well as melt curve analysis.

Representative melt curves for EGLN3, EGLN1 and IGFBP3 are shown in Figure 4.7. A representative real-time RT-PCR fluorescence amplification plot for EGLN3 is shown in Figure 4.8. Note that the curve in the representative amplification plot does not reach plateau as only 40 amplification cycles were performed, however, sequencing of purified PCR products confirmed that

each primer pair amplified the correct product.

Agarose gel electrophoresis photographs for the RT-PCR products of BNIP3, EGLN3, EGLN1, IGFBP2 and IGFBP3 are shown in Figure 4.9. Confirmation of sequence identity of the EGLN3 amplicon is shown in Figure 4.10.

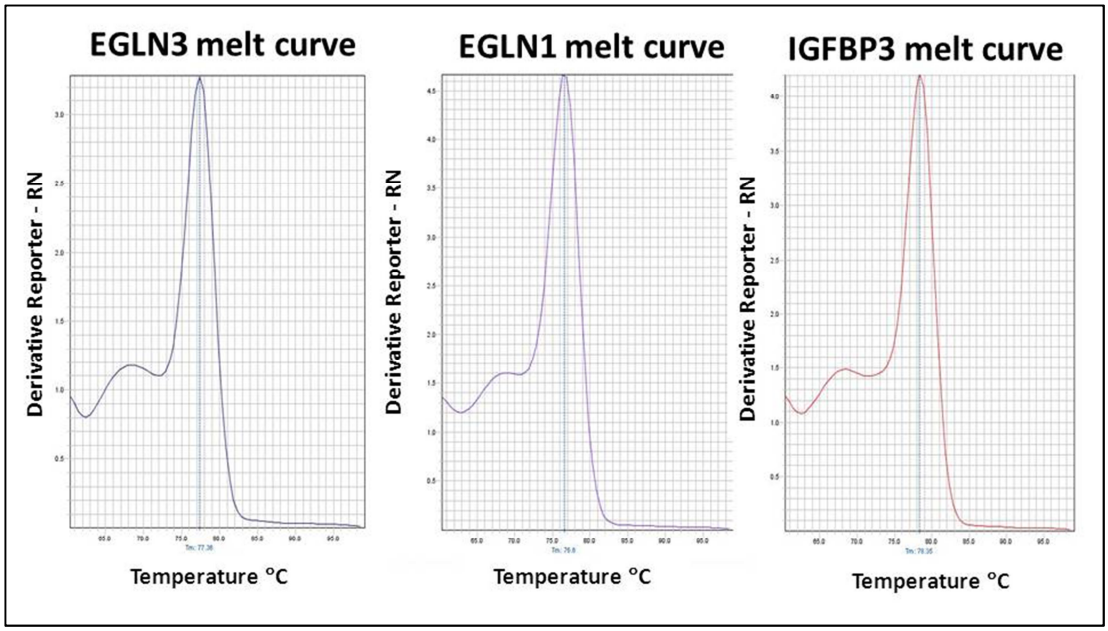

Figure 4.7 Melt curves of EGLN3, EGLN1 and IGFBP3 PCR products. The negative first-derivative of the normalised fluorescence generated by SYBR® Green during PCR amplification (y axis) is plotted against temperature (x axis). The products are subject to increasing temperatures to determine the melting temperature at which dissociation of double-stranded amplicon occurs and is associated with a loss of SYBR® Green fluorescence. The peak of the negative first-derivate plots show the temperature at which the change in fluorescence is at its maximum, corresponding with the melting temperature of the amplicon. Each plot has a well-defined peak, with a small shoulder preceding the peak. The height of the shoulder suggests a second product is not being amplified but may be a result of PCR conditions not being optimised. Sequencing of PCR results confirmed a single product was amplified from each gene that was identical to the sequence of the gene of interest. Melting temperatures: EGLN3 = 77.36°C; EGLN1= 77.6°C; IGFBP3 =78.35°C.

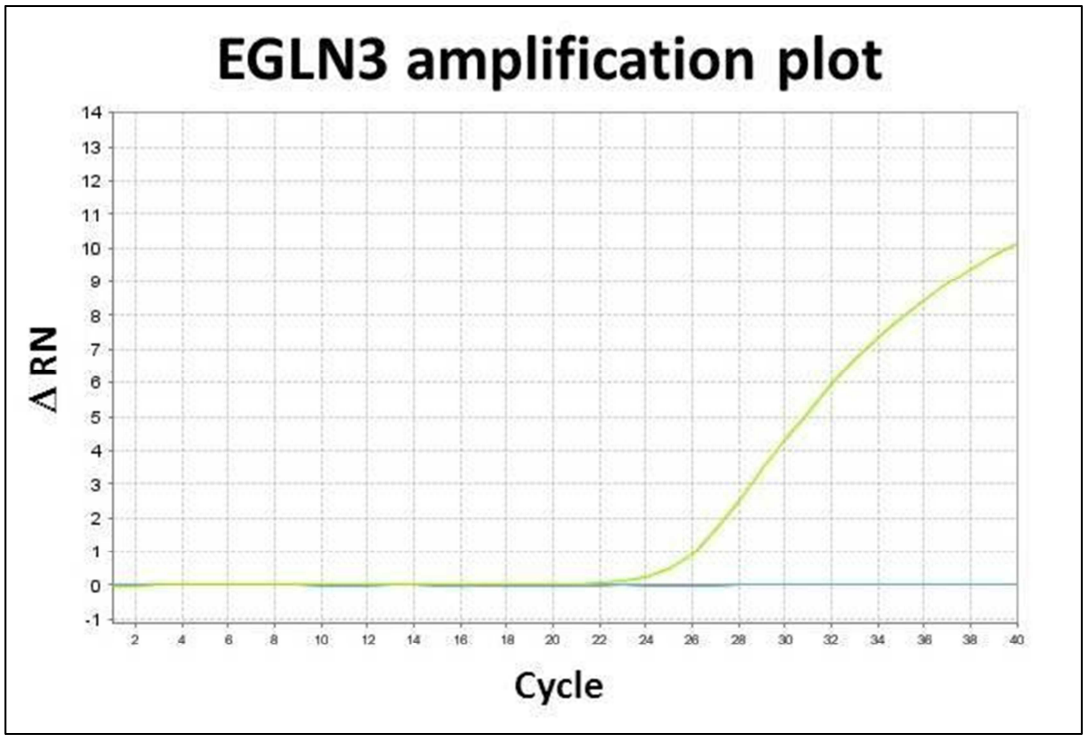

Figure 4.8 A representative real-time RT-PCR fluorescence amplification plot for EGLN3. The amplification plots change in SYBR® Green fluorescence on the y axis vs. each cycle of PCR product amplification on the x axis. The fluorescence of the reporter dye increases in proportion to the amplicon copy number. Quantification of gene expression is based on the number of cycles needed for the fluorescence of the reporter to exceed a manual threshold which is consistently set between each run. The earlier this occurs, the more abundant the transcript of the target gene is in the cDNA sample. The green line shows the amplification of the target gene in the standard pool sample. The blue line shows the standard pool reverse-transcriptase negative control which does not amplify any transcripts. The grey line (nearly invisible beneath the blue line) indicates the water non-template negative control which also does not show any amplification.

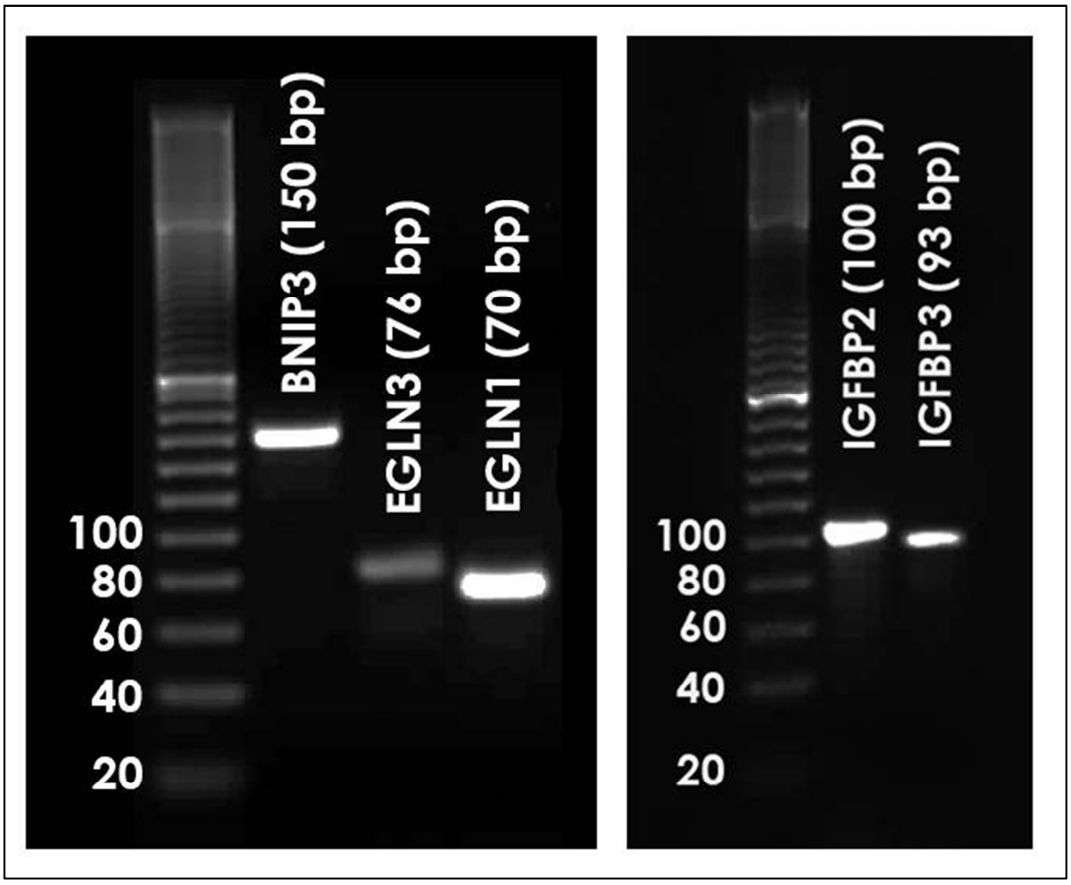

Figure 4.9 Agarose gel electrophoresis photographs of RT-PCR products of BNIP3, EGLN3, EGLN1, IGFBP2 and IGFBP3. PCR amplification products are shown for each gene of interest and found to be the expected size as shown in brackets. The agarose gel for BNIP3, EGLN3 and EGLN1, SCL16A3 and HK2 was performed by Rhys Fogarty (Department of Ophthalmology, Flinders University, SA, Australia), and the agarose gel for IGFBP2 and IGFBP3 performed by myself.

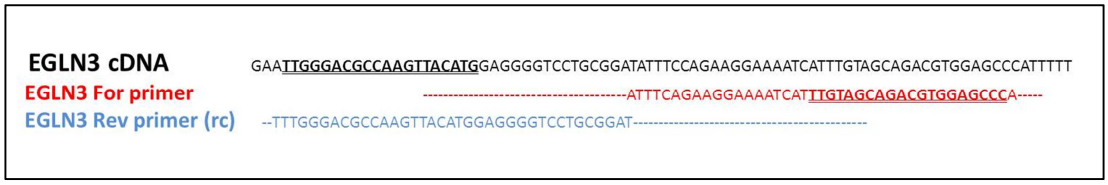

Figure 4.10 Confirmation of EGLN3 PCR product sequence to the EGLN3 amplicon. VectorNTI® software (Invitrogen, Carlsbad, CA, USA) was used to confirm sequence specificity of the PCR product to the EGLN3 amplicon. All PCR products showed sequence specificity to the amplicon of interest. Confirmation of BNIP3, EGLN3 and EGLN1, SCL16A3 and HK2 sequence verification were performed by Rhys Fogarty (Department of Ophthalmology, Flinders University, SA, Australia), and confirmation of IGFBP2 and IGFBP3 was performed by myself.

4.3.a.2 Determination of primer PCR amplification efficiencies

Primer PCR amplification efficiencies were determined for each set of primers using seven 1/5 v/v serial dilutions of the standard cDNA sample to generate a standard curve (section 2.4.l). The mean Ct value for each dilution was plotted against the log cDNA concentration (Figure 4.11) and the gradient of the regression line of the standard curve was used to calculate the primer PCR amplification efficiency as shown in Figure 4.12. The primer PCR amplification efficiencies for the 7 candidate genes are shown in Table 4.12. Amplification efficiencies were used in the quantification of gene expression [184].

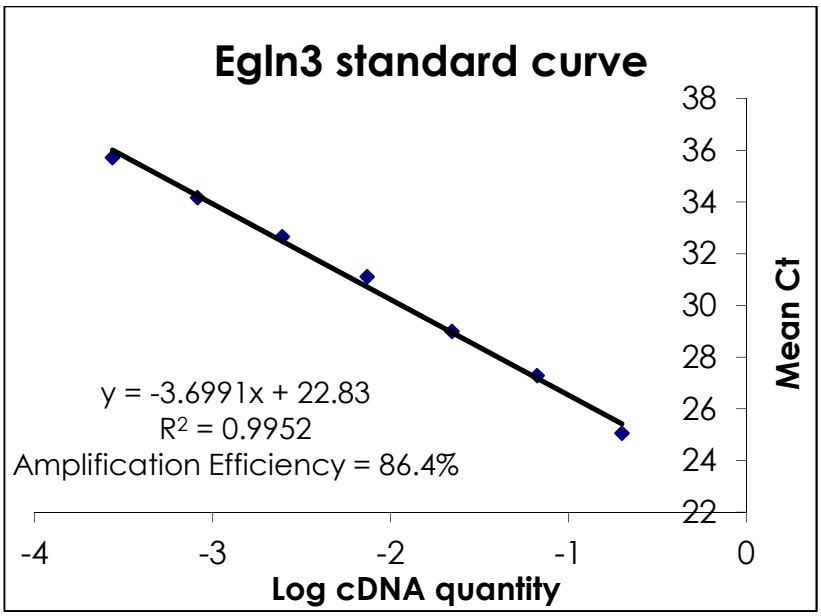

Figure 4.11 Standard curve for EGLN3 primer pair. Real-time RT-PCR was performed using seven 1/5 serial dilutions of the standard cDNA sample to generate a standard curve. The mean Ct values of triplicate wells for each dilution was plotted against the log cDNA concentration, where neat cDNA = 1. The gradient of the regression line, fitted to these points on the standard curve was used to calculate the primer PCR amplification efficiency.

Equation to determine PCR primer amplification efficiency

$$AE = [e^{(1/-g)}] - 1$$

AE = amplification efficiency, the change in fluorescence per cycle of PCR, expressed as a percentage. A 100% efficiency corresponds to a doubling of PCR product

e= Euler's number, as the natural logarithm [$\log_e$] was used to transform cDNA concentration values

g= gradient/slope of the standard curve regression line

Figure 4.12 The equation used to determine the PCR amplification efficiency of primer pairs as described by Meijerink et.al. [184]. This figure is a modified version of a figure derived from van Wijngaarden [181].

Primer pair	Amplification efficiency	R^2 value
EGLN3	86.4%	0.9952
EGLN1	55.0%	0.9924
SLC16A3	99.0%	0.9970
HK2	100.1%	0.9982
BNIP3	96.4%	0.9994
IGFBP2	102.3%	0.9991
IGFBP3	82.0%	0.9970

Table 4.12 Amplification efficiencies derived from the standard curve of candidate genes PCR primers. Mean Ct values of triplicate wells for each dilution was plotted against the log cDNA concentration and a regression line was fitted to these points. The slope of the regression line was used to determine the amplification efficiency, expressed as a percentage, using the equation shown in Figure 4.12. R^2 represents the fit of the regression line. It must be noted that IGFBP2 shows an amplification efficiency which is greater than 100%, which in reality is not possible, however, amplification efficiencies above 100% do occur and may reflect the overestimation of actual efficiency using this method [227, 237]. Determination of primer PCR amplification efficiencies for BNIP3, SCL16A3 and HK2 amplicon identity were performed by Rhys Fogarty (Department of Ophthalmology, Flinders University, SA, Australia). Determination of primer PCR amplification efficiencies of IGFBP2, IGFBP3, EGLN3 and EGLN1 were performed by myself.

4.3.b Confirmation of gene expression in pooled RNA

Quantitative real-time RT-PCR was performed on cDNA derived from the same RNA pools that were submitted for Affymetrix microarray analysis at day 3 to confirm the results of the microarray (section 2.4.q). These preliminary real-time RT-PCR experiments using the pooled RNA were kindly performed by Rhys Fogarty (Department of Ophthalmology, Flinders University, SA, Australia). Gene expression levels were determined relative to a standard pooled mRNA sample and were normalised against the two reference genes ARBP and HPRT as described in section 2.4.r.

Subsequent analysis of gene expression was performed by myself. The Shapiro-Wilk test for normality was used due to the small sample size of the replicate wells. Two-way analysis of variance (ANOVA) was then used to compare the effects of strain (F344 and SD together), treatment (room air and cyclic hyperoxia exposure together) and the interaction between strain and treatment (strain*treatment) on gene expression. The significance (alpha) level was set at 0.05 unless otherwise specified. Summary data were expressed as means with 95% confidence intervals (95% CI).

4.3.b.1 EGLN3 mRNA expression at day 3 in pooled RNA

EGLN3 was downregulated in F344 cyclic hyperoxia-exposed rats by 2.1 fold compared to F344 room air-exposed rats (Figure 4.13). EGLN3 was also downregulated in SD cyclic hyperoxia-exposed rats compared to SD room air

exposed rats to a greater extent (5.5 fold) compared to F344 cyclic hyperoxia exposed rats (2.0 fold) at day 3. The effect of strain (F344 and SD together) was not found to be statistically significant; however, the effect of treatment (room air and cyclic hyperoxia exposure together) was significant (Table 4.13). A statistically significant strain*treatment interaction was also observed at day 3 in response to hyperoxia. These data suggest there is a strain-dependent difference in EGLN3 expression at day 3.

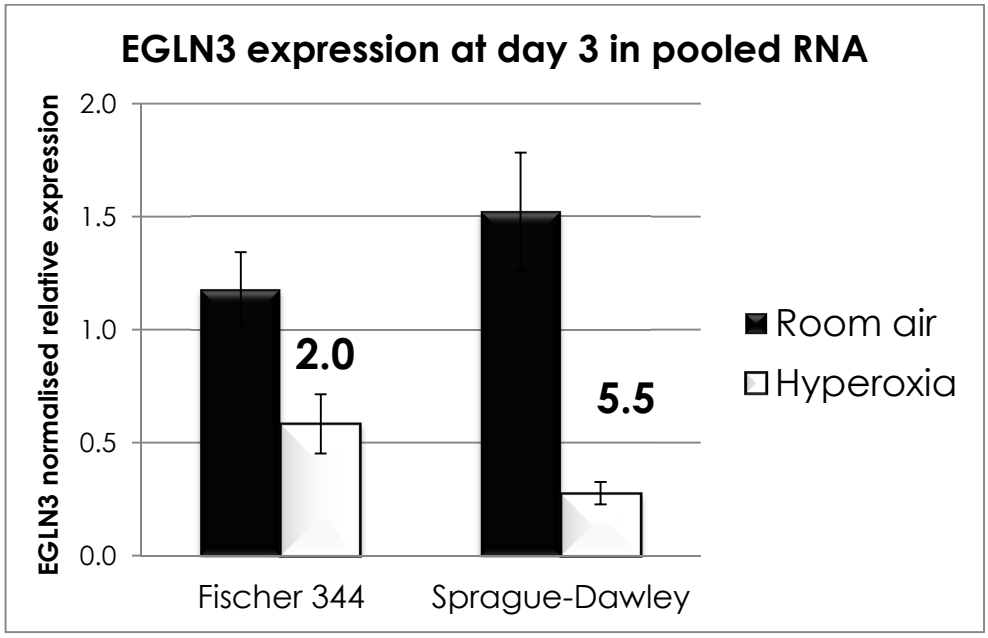

Figure 4.13 Retinal EGLN3 mRNA expression in F344 and SD pooled RNA at day 3 in response to hyperoxia. Quantification was performed on pooled RNA identical to those used in the microarray analysis. Error bars ± SD of 6 replicate wells. Relative expression levels were normalised to the reference genes ARBP and HPRT. Numbers above bars are fold changes by hyperoxia.

Variable	**Day 3**
Strain	F(1,24)=0.059, p=0.810
Treatment	F(1,24)= 180.512, p<0.001
Interaction Strain * Treatment	(F(1,24)=22.296, p<0.001

Table 4.13 Results from two-way ANOVA analysis for EGLN3 expression at day 3 in response to strain (F344 and SD rats together), treatment (room air and cyclic hyperoxia exposure together) and strain*treatment. The significance (alpha) level was set at 0.05. The effect of treatment was found to be statistically significant at day 3 in response to hyperoxia. A statistically significant strain*treatment interaction was also observed.

4.3.b.2 EGLN1 mRNA expression at day 3 in pooled RNA

EGLN1 was downregulated in F344 cyclic hyperoxia-exposed rats by 2.2 fold compared to F344 room air-exposed rats (Figure 4.14). EGLN1 was also downregulated in SD cyclic hyperoxia-exposed rats compared to SD room air exposed rats by 1.8 fold. The effect of strain (F344 and SD together), treatment (room air and cyclic hyperoxia exposure together) and the interaction between strain and treatment were found to be statistically significant at day 3 in response to hyperoxia (Table 4.14) These data suggest there is a strain-dependent difference in EGLN1 expression at day 3.

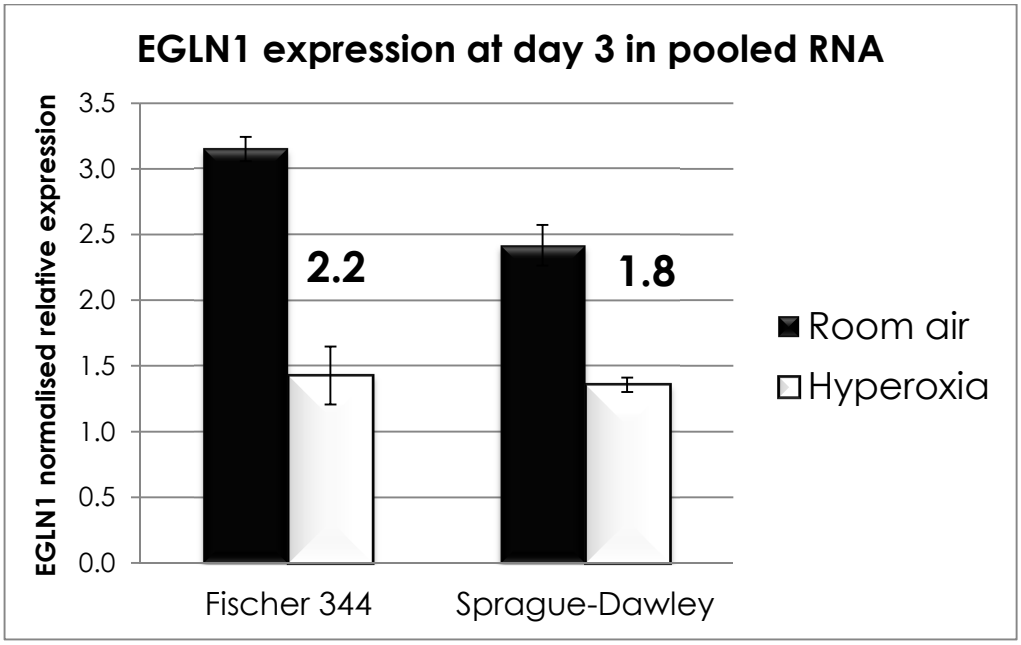

Figure 4.14 Retinal EGLN1 mRNA expression in F344 and SD pooled RNA at day 3 in response to hyperoxia. Quantification was performed on pooled RNA identical to those used in the microarray analysis. Error bars = ± SD of 6 replicate wells. Relative expression levels were normalised to the reference genes ARBP and HPRT. Numbers above bars are fold changes by hyperoxia.

Variable	**Day 3**
Strain	F(1,24)=27.615, p<0.001
Treatment	F(1,24)=316.860, p<0.001
Interaction Strain * Treatment	F(1,24)=7.747, p<0.05

Table 4.14 Results from two-way ANOVA analysis for EGLN1 expression at day 3 in response to strain (F344 and SD rats together), treatment (room air and cyclic hyperoxia exposure together) and strain*treatment. The significance (alpha) level was set at 0.05. The effect of strain, treatment and the strain*treatment interaction were all found to be statistically significant.

4.3.b.3 SLC16A3 mRNA expression at day 3 in pooled RNA

SLC16A3 was downregulated by 4.7 fold in F344 cyclic hyperoxia-exposed rats compared to F344 room air-exposed rats (Figure 4.15). SLC16A3 was also downregulated in SD cyclic hyperoxia-exposed rats compared to SD room air exposed rats to a greater extent (6.3 fold) at day 3. The results of the two-way ANOVA are shown in Table 4.15. Strain (F344 and SD together) and treatment (room air and cyclic hyperoxia exposure together) were independently found to have a statistically significant effect on SLC16A3 expression. However, the interaction between the two variables did not have a statistically significant effect at day 3 in response to hyperoxia.

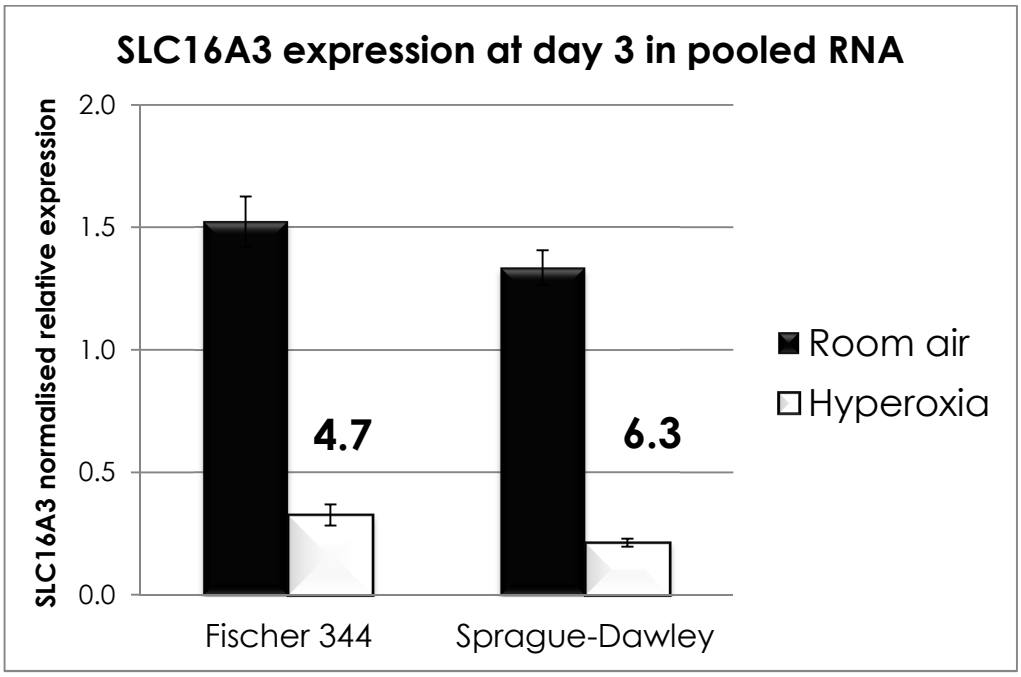

Figure 4.15 Retinal SLC16A3 mRNA expression in F344 and SD pooled RNA at day 3 in response to hyperoxia. Quantification was performed on pooled RNA identical to those used in the microarray analysis. Error bars ± SD of 6 replicate wells. Relative expression levels were normalised to the reference genes ARBP and HPRT. Numbers above bars are fold changes by hyperoxia.

Variable	Day 3
Strain	F(1,24)=29.616, p<0.001
Treatment	F(1,24)=1776.267, p<0.001
Interaction Strain * Treatment	F(1,24)=1.934, p=0.179

Table 4.15 Results from two-way ANOVA analysis for SLC16A3 expression at day 3 in response to strain (F344 and SD rats together), treatment (room air and cyclic hyperoxia exposure together) and strain*treatment. The significance (alpha) level was set at 0.01 as Levene's Test of Equality of Error Variances was significant, suggesting that the variance across all groups was not equal, therefore a more stringent significance level was set. The effect of strain and treatment were found to be statistically significant at day 3 in response to hyperoxia; however the interaction between strain and treatment was not.

4.3.b.4 HK2 mRNA expression at day 3 in pooled RNA

Expression of HK2 was downregulated in both strains in response to hyperoxia at day 3 as shown in Figure 4.16. HK2 was downregulated by 2.4 fold in F344 cyclic hyperoxia-exposed rats compared to room air-exposed rats. In SD rats, HK2 was downregulated to a greater extent by 4.5 fold in cyclic hyperoxia-exposed rats compared to room air-exposed controls. The results of the two-way ANOVA are shown in Table 4.16. Whilst strain did not have a statistically significant effect on SLC16A3 expression, treatment and the interaction between strain and treatment were found to be statistically significant at day 3.

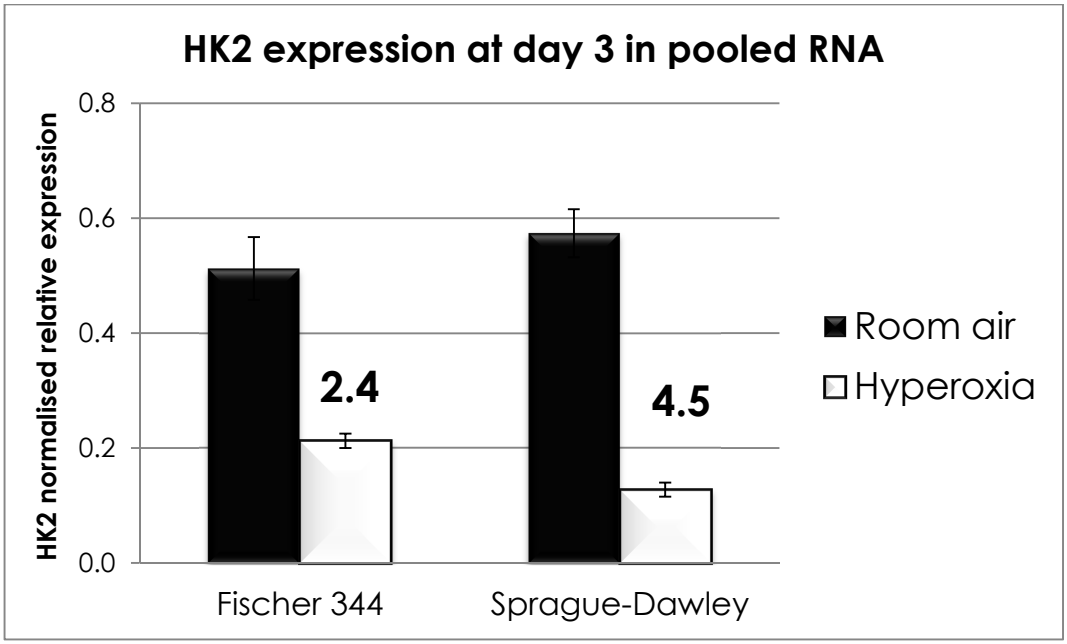

Figure 4.16 Retinal HK2 mRNA expression in F344 and SD pooled RNA at day 3 in response to hyperoxia. Quantification was performed on pooled RNA identical to those used in the microarray analysis. Error bars ± SD of 6 replicate wells. Relative expression levels were normalised to the reference genes ARBP and HPRT. Numbers above bars are fold changes by hyperoxia.

Variable	Day 3
Strain	F(1,24)=0.445, p=0.029
Treatment	F(1,24)=621.760, p<0.001
Interaction Strain * Treatment	F(1,24)=23.990, p<0.001

Table 4.16 Results from two-way ANOVA analysis for HK2 expression at day 3 in response to strain (F344 and SD rats together), treatment (room air and cyclic hyperoxia exposure together) and strain*treatment. The significance (alpha) level was set at 0.01 as Levene's Test of Equality of Error Variances was significant, suggesting that the variance across all groups was not equal, therefore a more stringent significance level was set. Treatment and the interaction between strain and treatment were found to have statistically significant effects on SLC16A3 expression in response to hyperoxia at day 3.

4.3.b.5 BNIP3 mRNA expression at day 3 in pooled RNA

BNIP3 was found to be downregulated in response to hyperoxia at day 3 in both strains as shown in Figure 4.17. BNIP3 was downregulated 2.6 fold in F344 cyclic hyperoxia-exposed rats compared to F344 room air-exposed rats. A greater reduction in BNIP3 expression was observed in SD cyclic hyperoxia-exposed rats compared to room air-exposed rats (3.6 fold). The effect of strain was not statistically significant however; the effect of treatment and the interaction between strain and treatment were found to be statistically significant (Table 4.17).

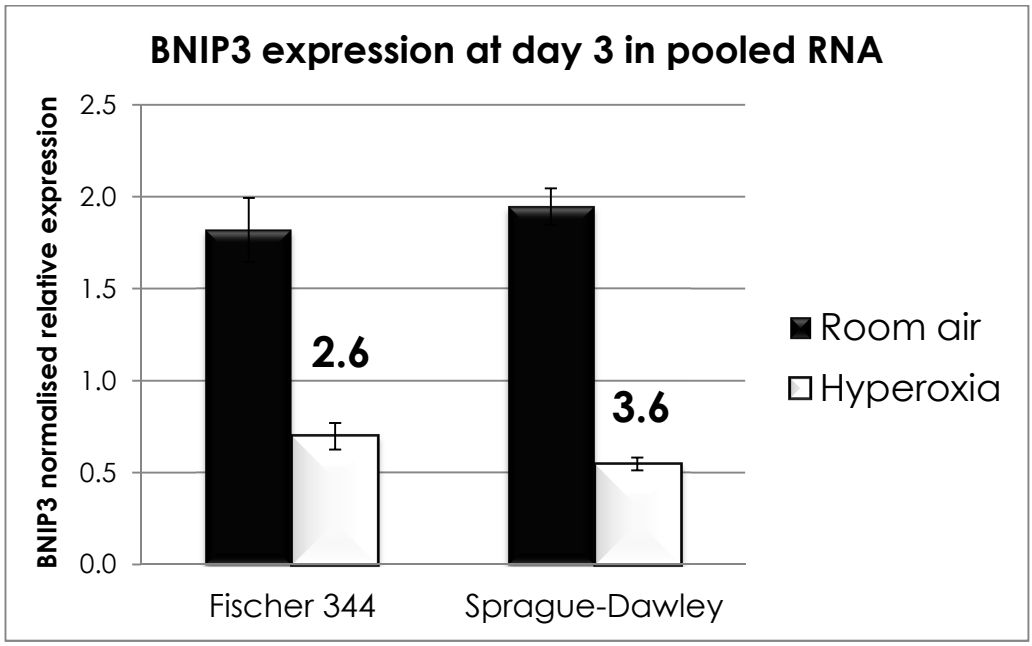

Figure 4.17 Retinal BNIP3 mRNA expression in F344 and SD pooled RNA at day 3 in response to hyperoxia. Quantification was performed on pooled RNA identical to those used in the microarray analysis. Error bars ± SD of 6 replicate wells. Relative expression levels were normalised to the reference genes ARBP and HPRT. Numbers above bars are fold changes by hyperoxia.

Variable	Day 3
Strain	F(1,24)=0.094, p=0.763
Treatment	F(1,24)=836.435, p<0.001
Interaction Strain * Treatment	F(1,24)=10.082, p<0.01

Table 4.17 Results from two-way ANOVA analysis for BNIP3 expression at day 3 in response to strain (F344 and SD rats together), treatment (room air and cyclic hyperoxia exposure together) and strain*treatment. The significance (alpha) level was set at 0.01 as Levene's Test of Equality of Error Variances was significant, suggesting that the variance across all groups was not equal, therefore a more stringent significance level was set. The effect of treatment and the interaction between strain and treatment were found to be statistically significant.

4.3.b.6 IGFBP2 mRNA expression at day 3 in pooled RNA

IGFBP2 was found to be downregulated in response to hyperoxia at day 3 in both strains as shown in Figure 4.18. IGFBP2 was downregulated 2.1 fold in F344 cyclic hyperoxia-exposed rats compared to F344 room air-exposed rats. The same fold decrease in IGFBP2 expression was observed in SD cyclic hyperoxia-exposed rats compared to room air-exposed rats. There was a statistically significant effect for treatment; however, the effect of strain and the interaction between strain and treatment were not statistically significant in terms of IGFBP2 expression (Table 4.18).

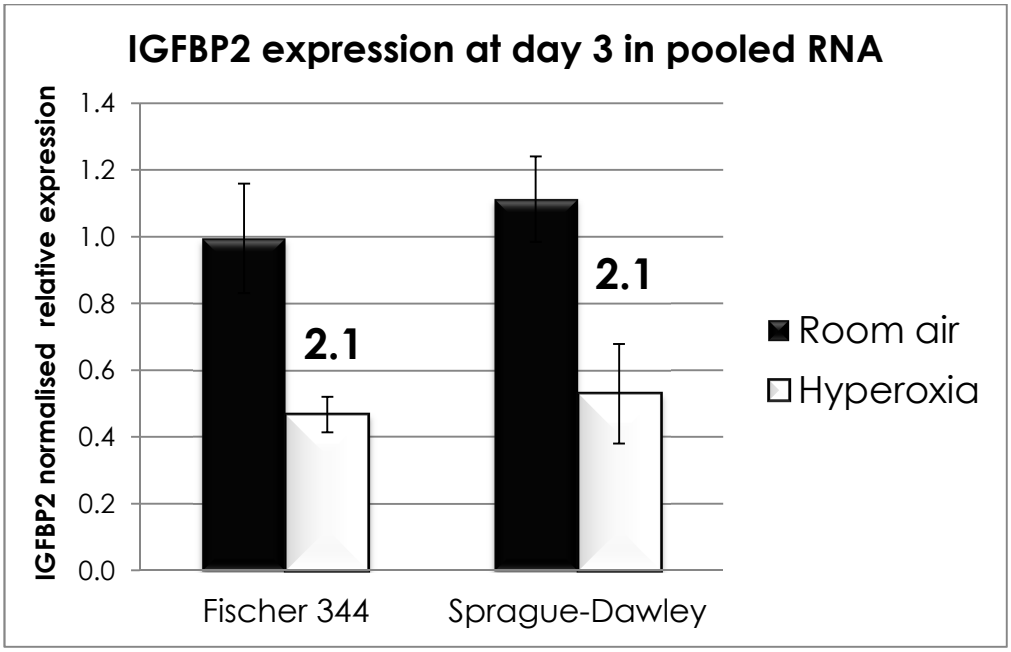

Figure 4.18 Retinal IGFBP2 mRNA expression in F344 and SD pooled RNA at day 3 in response to hyperoxia. Quantification was performed on pooled RNA identical to those used in the microarray analysis. Error bars = ± SD of 6 replicate wells. Relative expression levels were normalised to the reference genes ARBP and HPRT. Numbers above bars are fold changes by hyperoxia.

Variable	**Day 3**
Strain	F(1,24)=2.863, p=0.106
Treatment	F(1,24)=107.218, p<0.001
Interaction Strain * Treatment	F(1,24)=0.232, p=0.636

Table 4.18 Results from two-way ANOVA analysis for IGFBP2 expression at day 3 in response to strain (F344 and SD rats together), treatment (room air and cyclic hyperoxia exposure together) and strain*treatment. The significance (alpha) level was set at 0.05. The effect of treatment was found to be statistically significant at day 3 in response to hyperoxia.

4.3.b.7 IGFBP3 mRNA expression at day 3 in pooled RNA

IGFBP3 was found to be differentially expression in response to strain at day 3 (Figure 4.19). IGFBP3 was downregulated 2.1 fold in F344 cyclic hyperoxia-exposed rats compared to room air exposed rats. On the other hand, SD cyclic hyperoxia-exposed rats showed a 1.3 fold upregulation of IGFBP3 expression in response to hyperoxia. IGFBP3 expression was not significantly affected by strain or treatment. However, the interaction between strain*treatment was statistically significant (Table 4.19), suggesting there is a strain-dependent difference in IGFBP3 expression in response to hyperoxia at day 3.

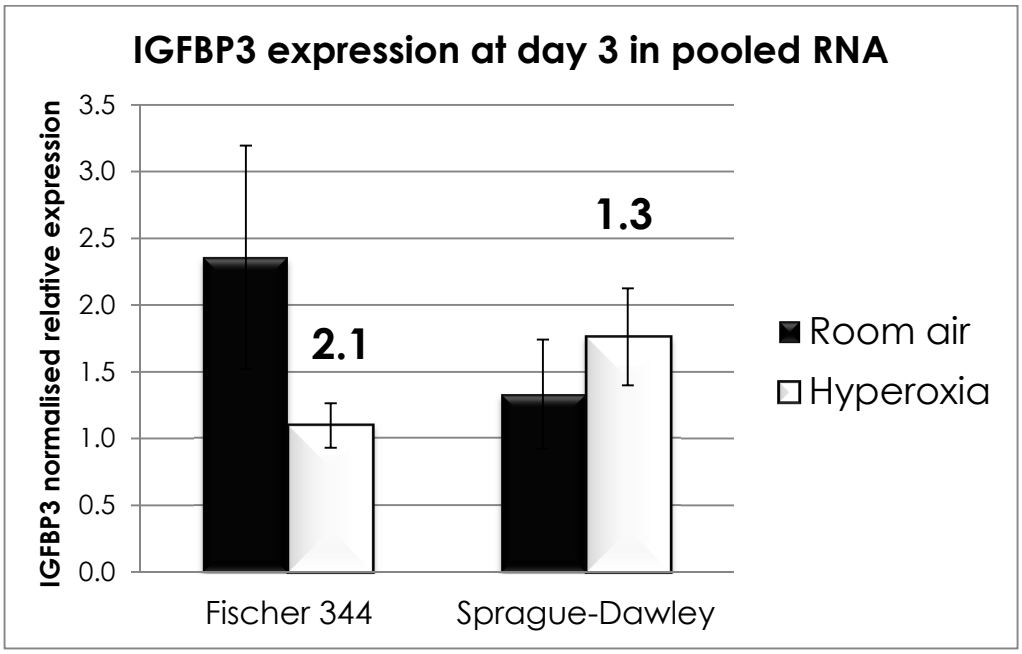

Figure 4.19 Retinal IGFBP3 mRNA expression in F344 and SD pooled RNA at day 3 in response to hyperoxia. Quantification was performed on pooled RNA identical to those used in the microarray analysis. Error bars = ± SD of 6 replicate wells. Note one replicate from the F344 cyclic hyperoxia-exposed samples was removed as an outlier prior to statistical analysis leaving 5 wells for analysis. Relative expression levels were normalised to the reference genes ARBP and HPRT. Numbers above bars are fold changes by hyperoxia.

Variable	Day 3
Strain	F(1,23)=0.980, p=0.335
Treatment	F(1,23)=3.160, p=0.091
Interaction Strain * Treatment	F(1,23)=14.270, p<0.01

Table 4.19 Results from two-way ANOVA analysis for IGFBP3 expression at day 3 in response to strain (F344 and SD rats together), treatment (room air and cyclic hyperoxia exposure together) and strain*treatment. An adjusted significance (alpha) level was set at 0.01 as the variance was not equal across all groups. The interaction between strain and treatment was found to be statistically significant.

4.3.c Confirmation of gene expression in individual rats

Subsequent time-course analysis of EGLN3, EGLN1 and IGFBP3 gene expression was performed at days 3, 5 and 6, in individual rats to determine the effect of intra-strain variation. EGLN3 and EGLN1 were chosen, given their role in regulating HIF-α. IGFBP3 was chosen as it showed a strain-dependent response to hyperoxia in the preliminary quantitative real-time RT-PCR experiments and has previously been associated with OIR. Five to 13 rats were analysed for each treatment group, depending on the quality of the total RNA used for cDNA synthesis. Any animal from which the RNA yield was poor or partially degraded was excluded from further analysis. Data were transformed where necessary to ensure data were normally distributed prior to statistical analysis using two-way analysis of variance (ANOVA). Two-way ANOVA was used to compare the effects of strain (F344 and SD

together), treatment (room air and cyclic hyperoxia exposure) and the interaction between strain and treatment (strain*treatment) on gene expression. The significance (alpha) level was set at 0.05 unless otherwise indicated.

4.3.c.1 EGLN3 mRNA expression

4.3.c.1.a EGLN3 mRNA expression at day 3

At day 3, EGLN3 expression was unchanged in F344 cyclic hyperoxia-exposed rats compared to room air-exposed rats (Figure 4.20). In contrast, SD rats showed a 3.2 fold downregulation of EGLN3 expression in cyclic hyperoxia-exposed rats compared to room air exposed rats.

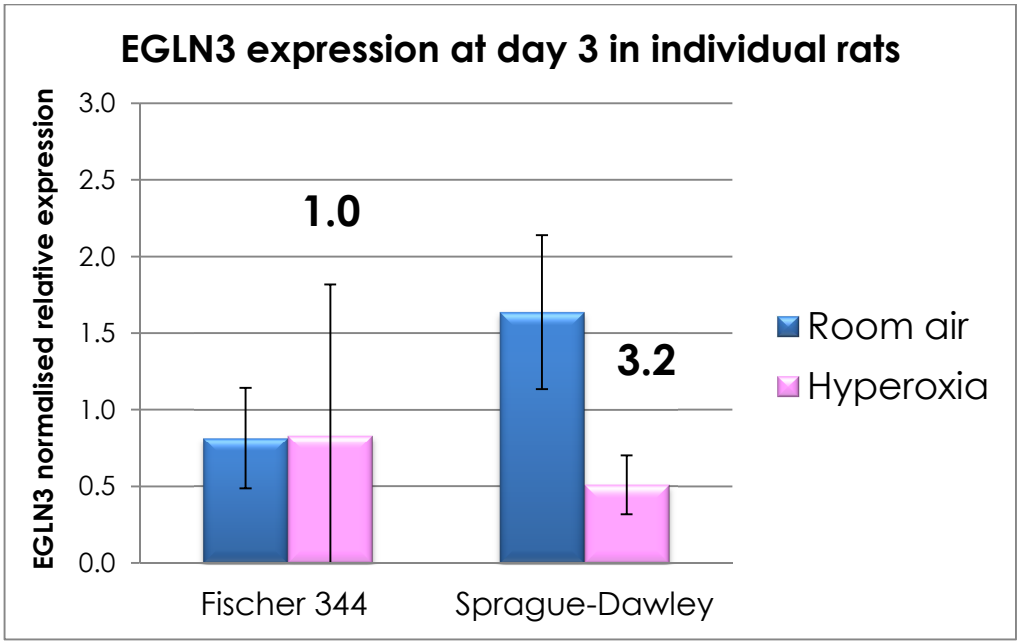

Figure 4.20 Retinal EGLN3 mRNA expression in F344 and SD rats at day 3 in response to hyperoxia. Quantification was performed on individual rats. Error bars ± SD; F344 room-air exposed n = 10; F344 cyclic hyperoxia-exposed n = 9; SD room air-exposed n = 9; SD cyclic hyperoxia-exposed n = 9. One cyclic hyperoxia-exposed SD rat was excluded from the data prior to statistical analysis due to a technical failure, leaving 9 cyclic hyperoxia-exposed SD rats. Data were log10 transformed prior to statistical analysis by two-way ANOVA. Relative expression levels were normalised to the reference genes ARBP and HPRT. Numbers above bars are fold changes in hyperoxia.

4.3.c.1.b EGLN3 mRNA expression at day 5

At day 5, EGLN3 was downregulated in F344 and SD cyclic hyperoxia-exposed rats by 2.2 fold and 1.9 fold, respectively compared to room air-exposed control rats (Figure 4.21).

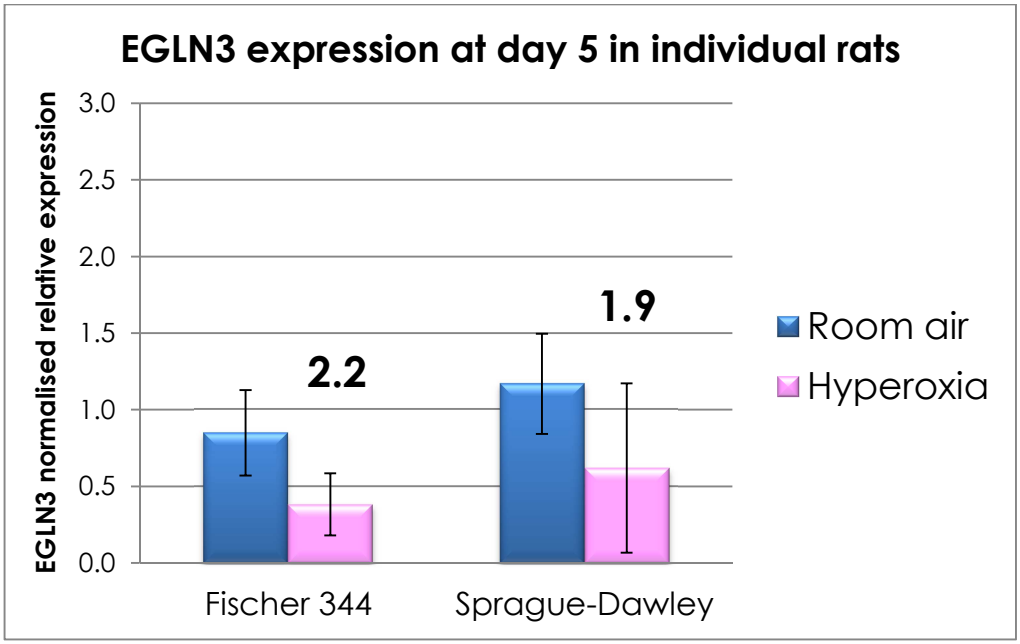

Figure 4.21 Retinal EGLN3 mRNA expression in F344 and SD rats at day 5 in response to hyperoxia. Quantification was performed on individual rats. Error bars ± SD; F344 room-air exposed n = 11; F344 cyclic hyperoxia-exposed n = 10; SD room air-exposed n = 9; SD cyclic hyperoxia-exposed n = 10. One cyclic hyperoxia-exposed SD rat was excluded from the data prior to statistical analysis due to a technical failure. A second cyclic hyperoxia-exposed SD rat considered an outlier during statistical analysis was also excluded, resulting in data from 8 cyclic hyperoxia-exposed SD rats being analysed. Relative expression levels were normalised to the reference genes ARBP and HPRT. Numbers above bars are fold changes in hyperoxia.

4.3.c.1.c EGLN3 mRNA expression at day 6

EGLN3 expression was upregulated 1.6 fold in response to relative hypoxia in cyclic hyperoxia-exposed F344 rats compared to F344 room air-exposed rats at day 6 in response to relative hypoxia. In comparison cyclic hyperoxia-exposed SD rats showed a 1.7 fold downregulation of EGLN3 expression compared to SD room air-exposed rats (Figure 4.22).

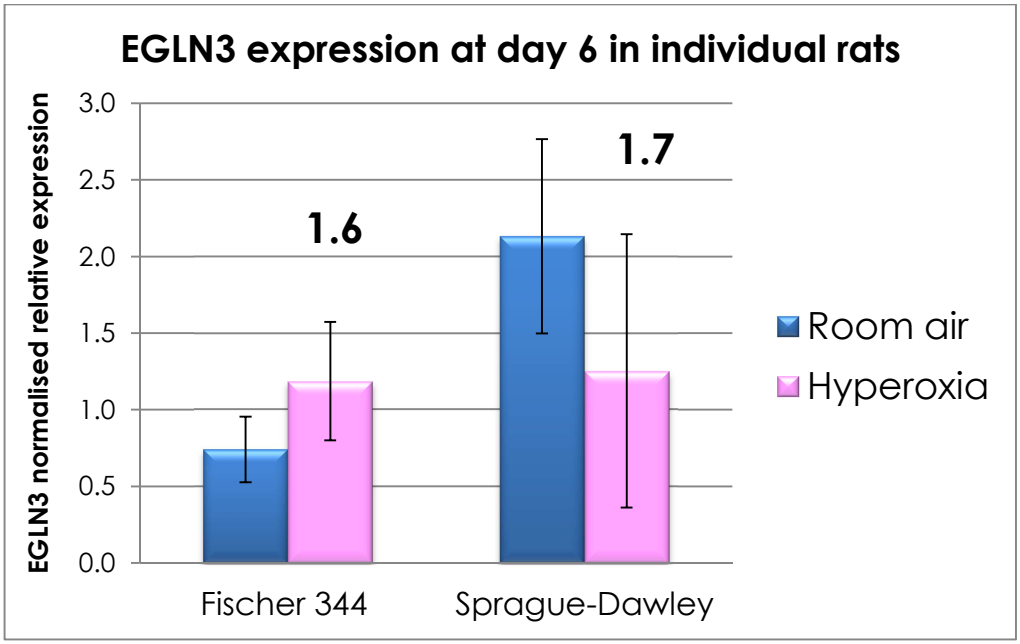

Figure 4.22 Retinal EGLN3 mRNA expression in F344 and SD rats at day 6 in response to hypoxia. Quantification was performed on individual rats. Error bars ± SD; F344 room-air exposed n = 13; F344 cyclic hyperoxia-exposed n = 7; SD room air-exposed n = 8; SD cyclic hyperoxia-exposed n = 10. Three SD room air control rats and 3 cyclic hyperoxia-exposed SD rat were excluded from the data prior to statistical analysis due to technical failures, leaving 5 SD room air-exposed rats and 7 SD cyclic hyperoxia-exposed rats for analyses. Data were log 10 transformed prior to statistical analysis by two-way ANOVA. Relative expression levels were normalised to the reference genes ARBP and HPRT. Numbers above bars are fold changes in hypoxia.

4.3.c.2 EGLN1 mRNA expression

4.3.c.2.a EGLN1 mRNA expression at day 3

EGLN1 expression remained relatively unchanged in response to hyperoxia at day 3 in both strain (Figure 4.23).

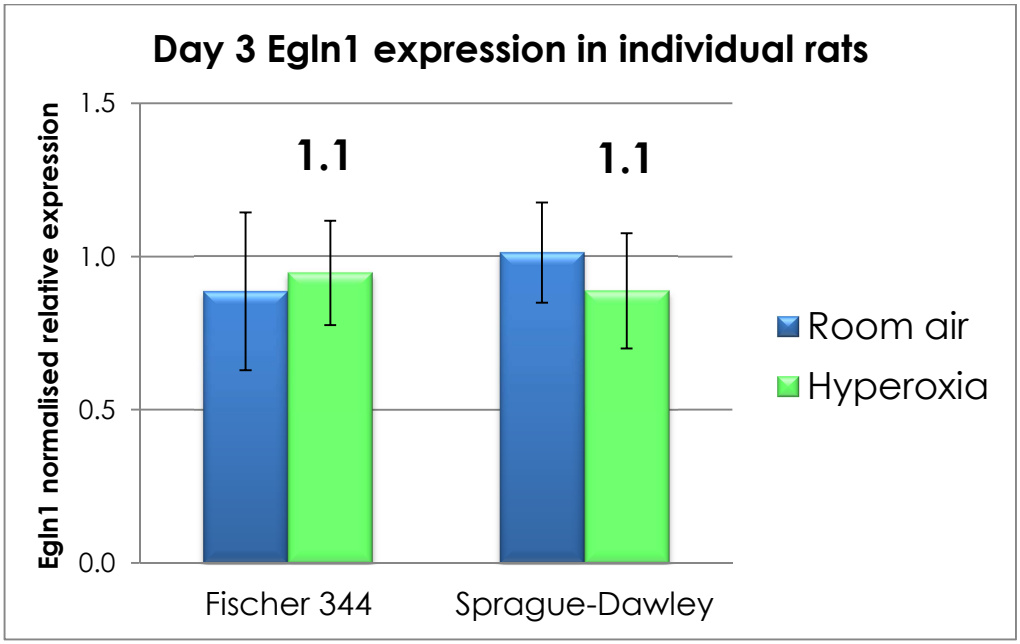

Figure 4.23 Retinal EGLN1 mRNA expression in F344 and SD rats at day 3 in response to hyperoxia. Quantification was performed on individual rats. Error bars ± SD; F344 room-air exposed n = 10; F344 cyclic hyperoxia-exposed n = 9; SD room air-exposed n = 9; SD cyclic hyperoxia-exposed n = 10. Note that one cyclic hyperoxia-exposed SD rat was excluded from the data prior to statistical analysis due to a technical failure. A second cyclic hyperoxia-exposed SD rat considered an outlier during statistical analysis was also excluded, resulting in data from 8 cyclic hyperoxia-exposed SD rats being analysed. Relative expression levels were normalised to the reference genes ARBP and HPRT. Numbers above bars are fold changes in hyperoxia.

4.3.c.2.b EGLN1 mRNA expression at day 5

Consistent with EGLN1 expression at day 3 in response to hyperoxia, at day 5, EGLN1 expression remained relatively unchanged in response to hyperoxia in both strains (Figure 4.24).

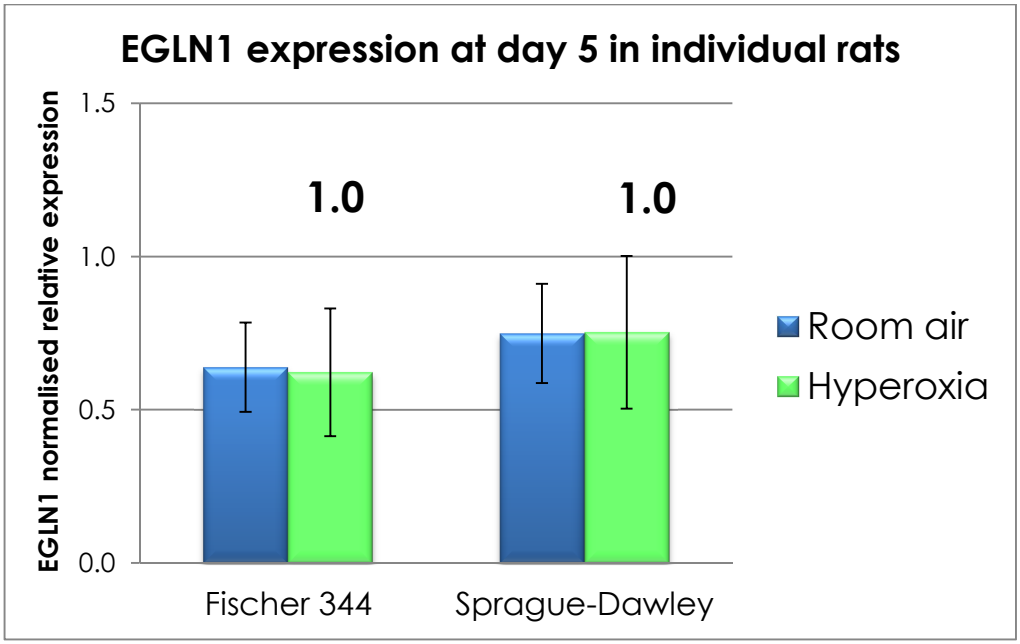

Figure 4.24 Retinal EGLN1 mRNA expression in F344 and SD rats at day 5 in response to hyperoxia. Quantification was performed on individual rats. Error bars ± SD; F344 room-air exposed n = 11; F344 cyclic hyperoxia-exposed n = 10; SD room air-exposed n = 9; SD cyclic hyperoxia-exposed n = 10. Note that one cyclic hyperoxia-exposed F344 rat and one SD rat were excluded from the data prior to statistical analysis due to technical failure. A second cyclic hyperoxia-exposed SD rat considered an outlier during statistical analysis was also excluded, resulting in data from 8 cyclic hyperoxia-exposed SD rats being analysed. Relative expression levels were normalised to the reference genes ARBP and HPRT. Numbers above bars are fold changes in hyperoxia.

4.3.c.2.c EGLN1 mRNA expression at day 6

EGLN1 expression was upregulated by 1.3 fold in F344 cyclic hyperoxia-exposed rats compared to room air-exposed control rats (Figure 4.25). In contrast, EGLN1 was regulated in the opposite direction, that is, there was a 1.3 fold downregulation of EGLN1 expression in SD cyclic hyperoxia-exposed rats compared to room air-exposed control rats. This suggests that

there is a strain-dependent differential expression of EGLN1 in response to relative hypoxia at day 6.

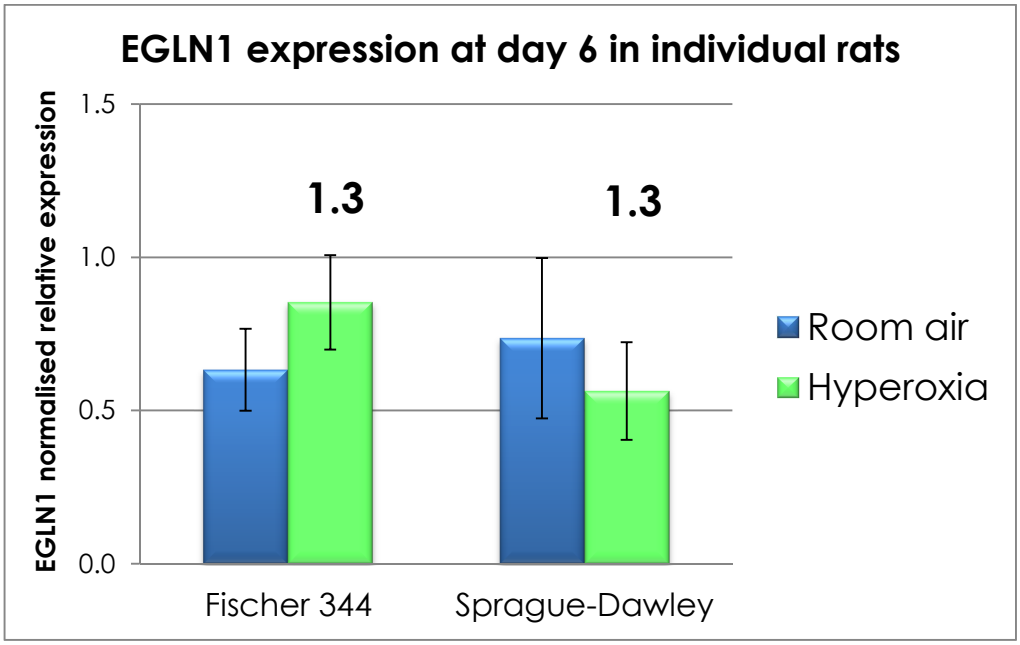

Figure 4.25 Retinal EGLN1 mRNA expression in F344 and SD rats at day 6in response to hypoxia. Quantification was performed on individual rats. Error bars ± SD; F344 room-air exposed n = 13; F344 cyclic hyperoxia-exposed n = 7; SD room air-exposed n = 5; SD cyclic hyperoxia-exposed n = 7. Note 2 cyclic hyperoxia-exposed SD rats were removed from statistical analysis as they were considered as outliers, leaving 5 cyclic hyperoxia-exposed SD rats for analysis. **Relative expression levels** were normalised to the reference genes ARBP and HPRT. Numbers above bars are fold changes in hypoxia.

4.3.c.3 IGFBP3 mRNA expression

4.3.c.3.a IGFBP3 mRNA expression at day 3

At day 3, IGFBP3 expression was largely unchanged in F344 cyclic hyperoxia-exposed rats compared to room air control rats (Figure 4.26). In

comparison, SD cyclic hyperoxia-exposed rats showed a 1.2 fold downregulation of IGFBP3 expression in response to hyperoxia.

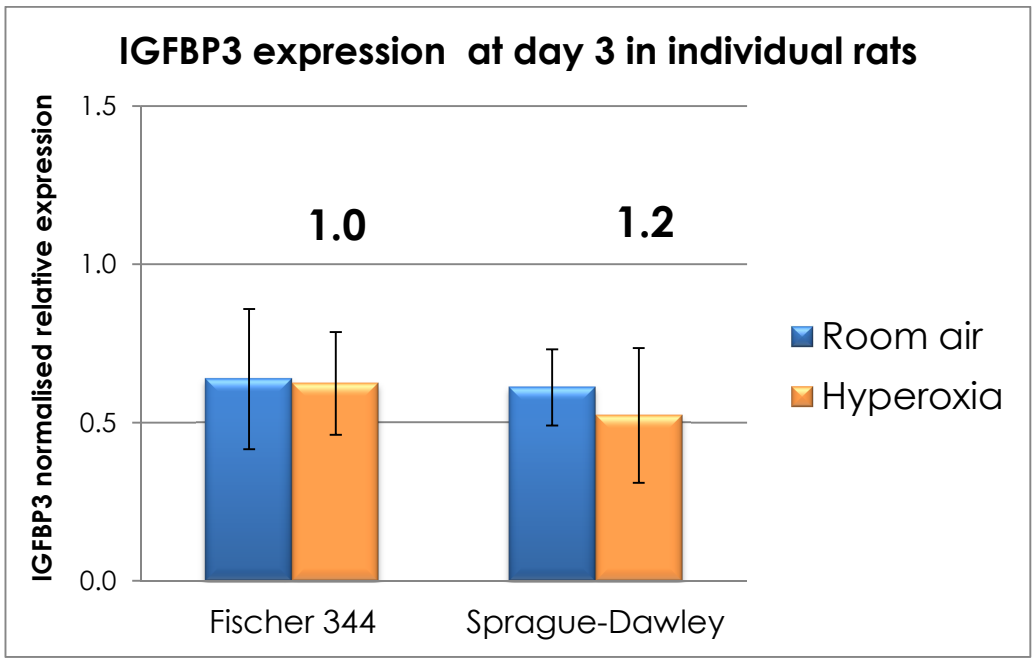

Figure 4.26 Retinal IGFBP3 mRNA expression in F344 and SD rats at day 3 in response to hyperoxia. Quantification was performed on individual rats. Error bars ± SD; F344 room-air exposed n = 10; F344 cyclic hyperoxia-exposed n = 9; SD room air-exposed n = 9; SD cyclic hyperoxia-exposed n = 10. One cyclic hyperoxia-exposed SD rat was excluded from the data prior to statistical analysis due to technical failure leaving 9 cyclic hyperoxia-exposed SD rats. Relative expression levels were normalised to the reference genes ARBP and HPRT. Numbers above bars are fold changes by cyclic hyperoxia.

4.3.c.3.b IGFBP3 mRNA expression at day 5

At day 5, IGFBP3 expression was downregulated in both strains in response to hyperoxia. F344 cyclic hyperoxia-exposed rats showed a 1.2 fold downregulation, whereas the fold change was slightly larger in the SD cyclic hyperoxia-exposed rats with a 1.4 fold downregulation (Figure 4.27).

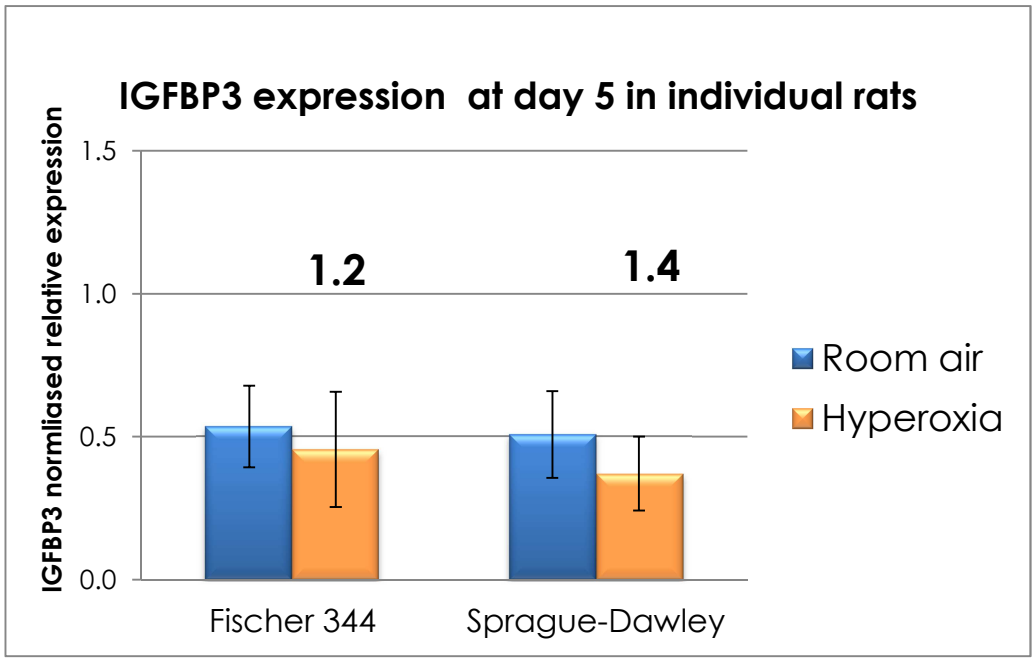

Figure 4.27 Retinal IGFBP3 mRNA expression in F344 and SD rats at day 5 in response to hyperoxia. Quantification was performed on individual rats. Error bars ± SD; F344 room-air exposed n = 11; F344 cyclic hyperoxia-exposed n = 10; SD room air-exposed n = 9; SD cyclic hyperoxia-exposed n = 10. One cyclic hyperoxia-exposed SD rat was excluded from the data prior to statistical analysis due to technical failure. A second cyclic hyperoxia-exposed SD rat was considered an outlier during statistical analysis was also excluded, resulting in data from 8 cyclic hyperoxia-exposed SD rats being analysed. Relative expression levels were normalised to the reference genes ARBP and HPRT. Numbers above bars are fold changes in hyperoxia.

4.3.c.3.c IGFBP3 mRNA expression at day 6

In response to relative hypoxia at day 6, IGFBP3 expression was relatively unchanged in F344 cyclic hyperoxia-exposed rats compared to room air-exposed rats (Figure 4.28). In contrast, SD cyclic hyperoxia-exposed rats showed a 2.5 fold downregulation of IGFBP3 expression in response to relative hypoxia.

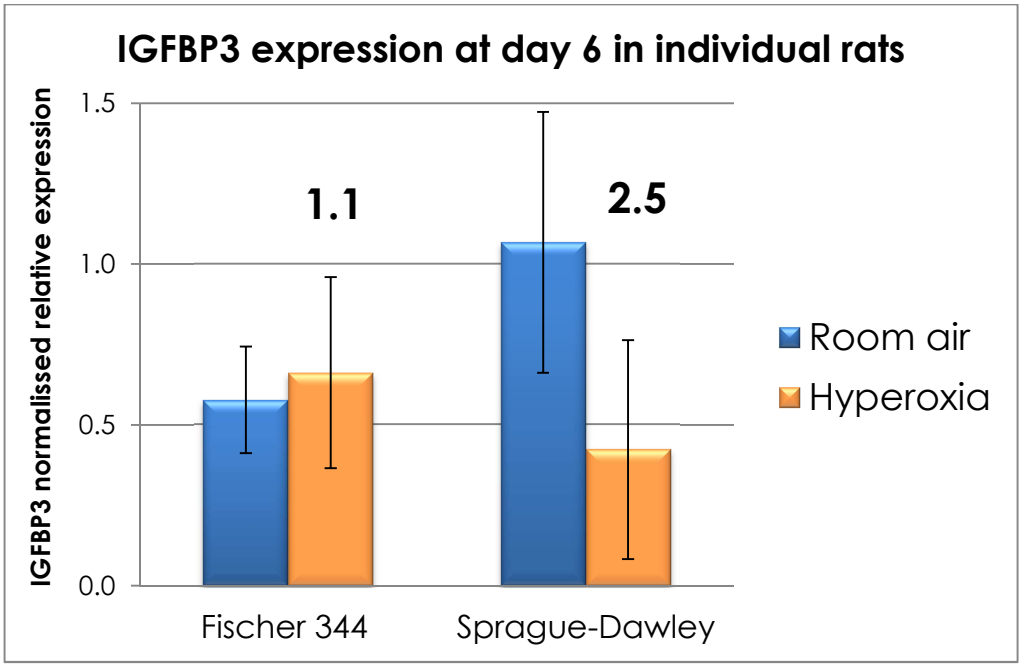

Figure 4.28 Retinal IGFBP3 mRNA expression in F344 and SD rats at day 6 in response to hypoxia. Quantification was performed on individual rats. Error bars ± SD; F344 room-air exposed n = 13; F344 cyclic hyperoxia-exposed n = 7; SD room air-exposed n = 8; SD cyclic hyperoxia-exposed n = 10. Three SD room air control rats and 3 cyclic hyperoxia-exposed SD rats were excluded from the data prior to statistical analysis due to technical failures, leaving 5 SD room air-exposed and 7 SD cyclic hyperoxia-exposed rats for statistical analyses. Data were square root transformed prior to statistical analysis by two-way. Relative expression levels were normalised to the reference genes ARBP and HPRT. Numbers above bars are fold changes by hypoxia.

4.3.d Summary of EGLN3, EGLN1 and IGFBP3 expression in individual rats at days 3, 5 and 6

4.3.d.1 Summary of EGLN3 expression at days 3, 5, and 6

A graph summarising expression of EGLN3 in F344 and SD rats in response to hyperoxia and relative hypoxia is shown in Figure 4.29. Overall, EGLN3 expression was unchanged in cyclic hyperoxia-exposed F344 rats at day 3 in response to hyperoxia but was downregulated in SD rats. At day 5, both

strains showed downregulation of EGLN3 in response to hyperoxia. A statistically significant (p=0.001) strain*treatment interaction was observed at day 3 (Table 4.20). At day 6, EGLN3 is regulated in a strain-dependent manner and is upregulated in response to relative hypoxia in F344 rats 1.6 fold but downregulated in SD rats 1.7 fold. The interaction between strain and treatment at day 6 is also significant (p=0.001).

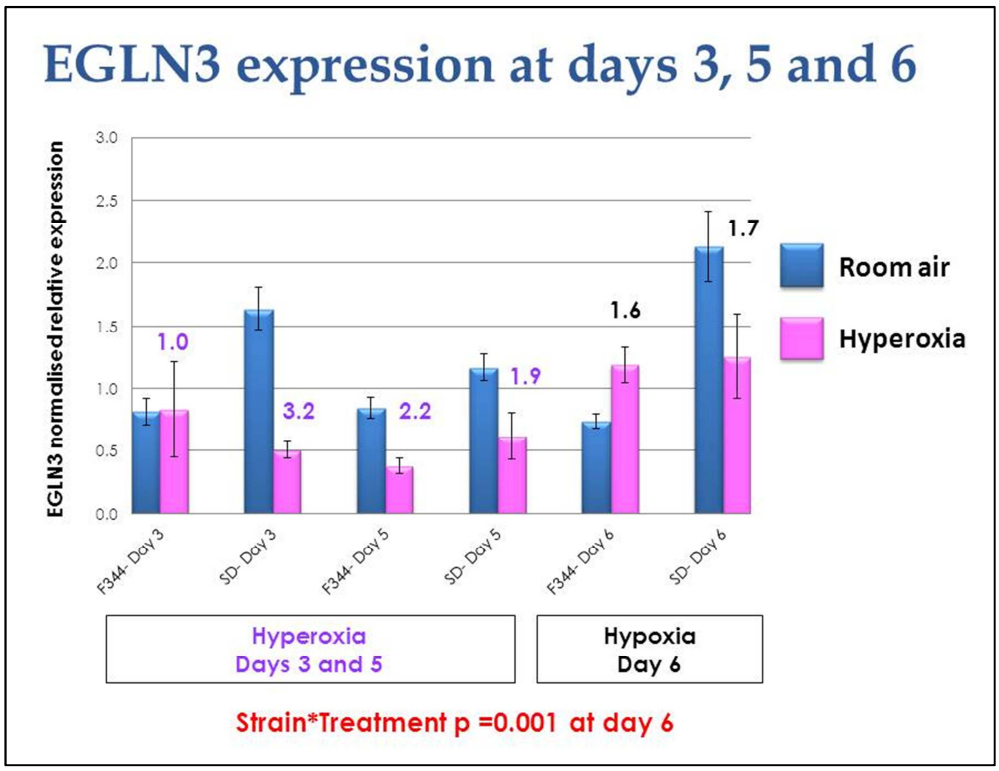

Figure 4.29 Summary of EGLN3 expression at days 3, 5 and 6 in response to cyclic hyperoxia. Quantification was performed on individual rats. Error bars ± SD. Statistical analysis was performed using two-way ANOVA. Data were transformed where necessary. Relative expression levels were normalised to the reference genes ARBP and HPRT. Numbers above bars are fold changes by exposure to cyclic hyperoxia.

Variable	Day 3	Day 5	Day 6
Strain	F(1,36)=0.366, p=0.549	F(1,39)=5.907, p<0.05	F(1,32)=15.388, p=0.001
Treatment	F(1,36)=11.237, p<0.01	F(1,39)=19.696, p<0.001	F(1,32)=0.043, p=0.838
Interaction Strain * treatment	F(1,36)=12.082, p= 0.001	F(1, 39)=0.128, p=0.723	F(1,32)=12.591, p=0.001

Table 4.20 Summary of the results from two-way ANOVA analysis for EGLN3 expression at days 3, 5 and 6 in response to strain, treatment and strain*treatment. Significance (alpha) level was set at 0.05. A statistically significant strain*treatment interaction was observed in response to hyperoxia at day 3, and in response to relative hypoxia at day 6.

4.3.d.2 Summary of EGLN1 expression at days 3, 5, and 6

A graph summarising EGLN1 expression in F344 and SD rats in response to hyperoxia and relative hypoxia is shown in Figure 4.30. Confirmation of EGLN1 expression in RNA pools used in the Affymetrix microarray showed EGLN1 was downregulated in response to hyperoxia at day 3 by 2.2 fold in F344 rats, compared to a 1.9 fold downregulation in SD rats. Quantitative real-time RT-PCR performed on individual animals however, showed EGLN1 expression was unchanged in response to hyperoxia at days 3 and 5 in both strains. At day 6, EGLN1was upregulated 1.3 fold in response to relative hypoxia in F344 rats but was downregulated by 1.3 fold in SD rats. At day 6, the strain*treatment interaction was statistically significant (p=0.006; Table 4.21).

Variable	Day 3	Day 5	Day 6
Strain	F(1,36)=0.256, p=0.617	F(1,37)=3.578, p=0.067	F(1,30)=1.967, p=0.172
Treatment	F(1,36)=0.231, p=0.634	F(1,37)= 0.011, p=0.918	F(1,30)=0.134, p=0.717
Interaction Strain * Treatment	F(1,36)=1.912, p=0.176	F(1,37)=0.026, p=0.873	F(1,30)=8.826, p<0.01

Table 4.21 Summary of the results from two-way ANOVA analysis for EGLN1 expression at days 3, 5 and 6 in response to strain, treatment and strain*treatment. Significance (alpha) level was set at 0.05. A statistically significant strain*treatment interaction was observed in response to relative hypoxia at day 6.

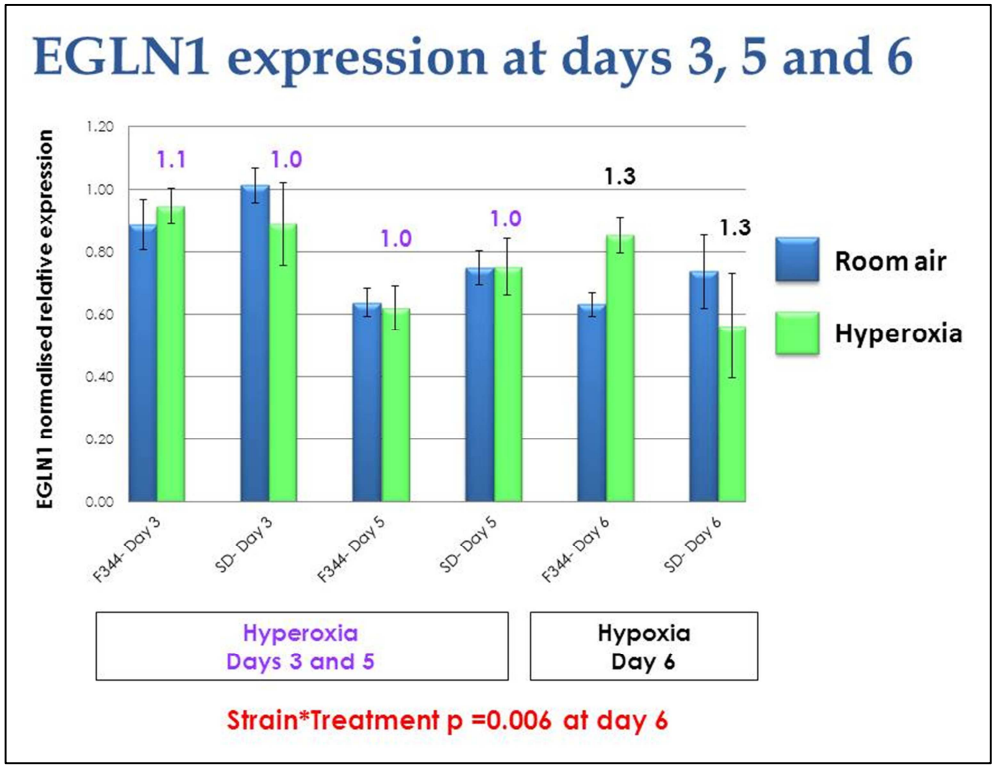

Figure 4.30 Summary of EGLN1 expression at days 3, 5 and 6 in response to cyclic hyperoxia. Quantification was performed on individual rats. Error bars ± SD. Statistical analysis was performed using two-way ANOVA. Data were transformed where necessary. Relative expression levels were normalised to the reference genes ARBP and HPRT. Numbers above bars are fold changes by exposure to cyclic hyperoxia.

4.3.d.3 Summary of IGFBP3 expression at days 3, 5, and 6

A graph summarising expression of IGFBP3 in F344 and SD rats in response to hyperoxia and relative hypoxia is shown in Figure 4.31. Confirmation of the results of the Affymetrix microarrays showed that IGFBP3 was differentially regulated in a strain-dependent manner in F344 and SD rats in response to hyperoxia. IGFBP3 was downregulated 2.1 fold in F344 rats, but was upregulated by 1.3 fold in SD rats. Quantitative real-time RT-PCR performed on individual animals showed IGFBP3 was unchanged in response to hyperoxia in F344 rats at day 3, but was downregulated in SD rats by 1.2 fold. IGFBP3 was downregulated in both strains by hyperoxia at day 5. At day 6, IGFBP3 expression remained largely unchanged in response to relative hypoxia in F344 rats but was downregulated 2.5 fold in SD rats. A statistically significant ($p=0.002$) strain*treatment interaction was observed at day 6 (Table 4.22).

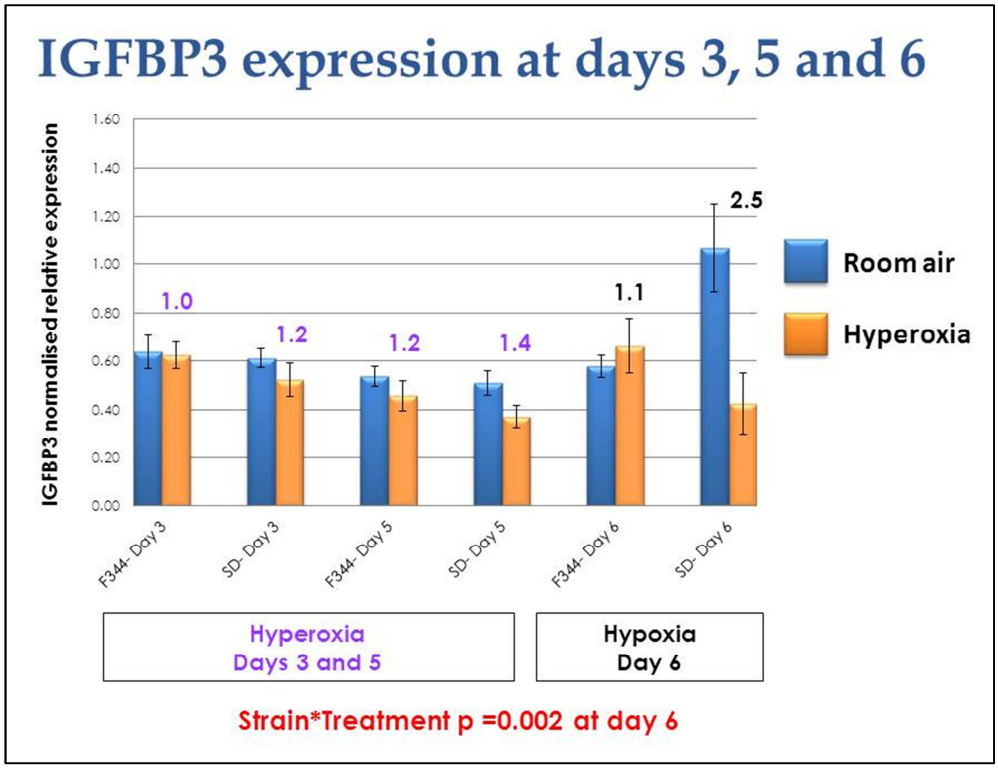

Figure 4.31 Summary of IGFBP3 expression at days 3, 5 and 6 in response to cyclic hyperoxia. Quantification was performed on individual rats. Error bars ± SD. Statistical analysis was performed using two-way ANOVA. Data were transformed where necessary. Relative expression levels were normalised to the reference genes ARBP and HPRT. Numbers above bars are fold changes by exposure to cyclic hyperoxia.

Variable	Day 3	Day 5	Day 6
Strain	F(1,37)=1.111, p=0.300)	F(1,38)=1.152, p=0.219	F(1,32)=0.748, p=0.394
Treatment	F(1,37)= 0.368, p=0.695	F(1,38)=4.315, p<0.05	F(1,32)=6.745, p<0.05
Interaction Strain * Treatment	F(1,37)=0.407, p=0.528	F(1,38)=0.289, p=0.594	F(1,32)=11.851, p<0.01

Table 4.22 Summary of the results from two-way ANOVA analysis for IGFBP3 expression at days 3, 5 and 6 in response to strain, treatment and strain*treatment. Significance (alpha) level was set at 0.05. A statistically significant strain*treatment interaction was observed in response to relative hypoxia at day 6.

4.4 DISCUSSION

4.4.a Summary of findings

My aim in this chapter was to use Affymetrix microarrays to investigate changes in retinal mRNA expression in two strains of rats which differ in their response to oxygen therapy, and to determine at which time point these changes were occurring. These changes may contribute to the different susceptibilities to OIR exhibited by albino inbred F344 and SD rats.

Using microarray analysis, a total of 888 genes were found to be differentially expressed to a statistically significant extent across all comparisons made at all 3 time points. Filtering this list of 888 genes based on statistically significant changes in gene expression which occurred in response to cyclic hyperoxia exposure in a strain-dependent manner resulted in 127 genes found to be differentially expressed to a statistically significant extent. Given it was not possible to confirm the results of the initial microarray screens for all 127 genes, functional annotation of differentially expressed genes was performed to identify genes which may be directly involved in differential susceptibility to OIR.

Functional annotation of genes differentially expressed in F344 and SD rats in response to hyperoxia at day 3 identified 7 genes of interest: EGLN3, EGLN1, SLC16A3, HK2, BNIP3, IGFBP2 and IGFBP3, which were all found to be downregulated in response to cyclic hyperoxia. Three genes considered

most likely to be involved in the development of OIR in the rat were chosen to confirm the microarray findings, using quantitative real-time RT-PCR. Time-course analysis of EGLN3, EGLN1 and IGFBP3 gene expression in individual rats at days 3, 5, and 6 was performed. EGLN3 and EGLN1 were chosen as they belong to a class of oxygen-dependent enzymes of HIF prolyl hydroxylases (PHDs) which regulate expression of HIF-α [233]. IGFBP3 was chosen as it has previously been associated with OIR [236].

Day 6 was the time point at which most genes were found to be differentially expressed to a statistically significant extent. In fact, 728 genes were found to be differentially expressed to a significant level as a result of strain differences alone, suggesting these changes may be in part due to developmental changes occurring in the retina with increasing age of the rats. However, there were also strain-dependent changes in gene expression occurring in response to relative hypoxia at day 6. Statistically significant interactions between strain and treatment were found to occur in response to relative hypoxia at day 6. EGLN3 was upregulated in response to relative hypoxia in resistant F344 rats but was downregulated in susceptible SD rats. Similarly, EGLN1 was also upregulated in response to relative hypoxia at day 6 in F344 rats, but was downregulated in SD rats. IGFBP3 also showed strain-dependent differential expression in response to relative hypoxia, with stable expression observed in F344 rats and downregulation of IGFBP3 seen in SD rats. As a result of these analyses, I propose that day 6 is a critical time

point for changes in gene expression to occur in response to relative hypoxia. The fact that these changes occur in a strain-dependent manner, and that these genes are regulated by oxygen, which is central to the pathogenesis of OIR, suggests they may also contribute to the differential susceptibility to OIR exhibited by resistant F344 and susceptible SD rats.

4.4.b. Microarray analysis of differential gene expression in the early stages of OIR

Little is known about the changes in gene expression that occur at early time points in OIR. At day 3, phenotypic evidence of strain-dependent differences in gene expression was apparent in F344 (resistant to OIR) and SD rats (sensitive to OIR) in response to hyperoxia as shown in Figure 4.3. However, the results of the microarray analysis showed that few genes in either strain that were regulated by exposure to cyclic hyperoxia at days 3, 5 and 6 reached statistical significance after correction for multiple comparisons. Microarrays were used as a means to screen large numbers of genes simultaneously within samples to look for differentially expressed genes and subsequent statistical analysis provided a method for prioritising candidates. It is possible that whilst genes that were regulated by exposure to cyclic hyperoxia did not reach statistical significance, changes in their expression levels may still have a significant biological effect. Changes in gene expression as small as 1.5 fold have previously been found to have a biological effect [228-230]. At day 3, 7 genes that showed relevance to OIR

were identified to be downregulated at least 1.5 fold by hyperoxia (Table 4.7). Whilst other genes at days 3, 5 and 6 also showed regulation by hyperoxia (Tables 4.7, 4.8 and 4.10), they did not appear to be directly relevant to OIR, therefore they were not investigated any further.

Quantitative real-time RT-PCR was used to confirm microarray results either using RNA pooled from 3 separate rats at day 3 or on RNA from individual rats at days 3, 5 and 6. Results from experiments performed on the same RNA pools used in the Affymetrix microarrays performed at day 3 were slightly different to the results from the arrays. Fold changes in EGLN3, SLC16A3, HK2 and BNIP3 expression measured by quantitative real-time RT-PCR in both strains were greater than the fold changes observed from the microarray data. In all cases, the direction of the fold change remained the same. Differences in microarray and quantitative real-time RT-PCR data used to confirm results from an array is not uncommon [238], and reinforces the need to validate results of microarrays using an alternate method.

Results from experiments performed on the pooled RNA were also found to be slightly different from those performed on RNA from individual rats and may be a result of the small number of rats (n =3) used in the microarray screen and the fact that the RNA from the retinae these rats were pooled. A larger number of individual rats (n=5-13 per treatment group) were used in subsequent analyses to confirm the results of the microarray screen,

introducing effects from intra-animal variation.

4.4.c Biological interpretation of strain-dependent differences in gene expression in response to cyclic hyperoxia and susceptibility to OIR

4.4.c.1 Expression of SLC16A3, HK2 and BNIP3 in response to cyclic hyperoxia

SLC16A3, HK2 and BNIP3 were downregulated in both strains in response to hyperoxia at day 3. SLC16A3 is involved in the transport of monocarboxylates such as pyruvate and lactate across cell membranes and is known to be expressed in ocular tissues including the retina [239]. SLC16A3 helps to rapidly export lactate, the end product of glycolysis, out of retinal cells and prevent intracellular acidosis [239]. It has been hypothesized that loss of SLC16A3 and other monocarboxylate transporters may compromise glucose metabolism and result in abnormalities in retinal function and retinal degeneration [240]. HK2 is involved in glycolysis and has previously been reported to be upregulated by hypoxia [235]. BNIP3 is a member of the Bcl-2 family of proteins that play a role in apoptosis [234]. BNIP3 has been found to be expressed in rat retinal ganglion cells *in vitro*, and a homolog of BNIP3, nip3a, has been found in the zebrafish retina [241, 242]. In normoxic conditions, BNIP3 expression is suppressed by the tumour suppressor p53 [242]. Expression of the zebrafish homolog nip3a is induced by hypoxia, and expression was further enhanced by the knockdown of p53, resulting in

enhanced cell death. Studies in human cell lines and p53 mutant/knockdown zebrafish embryos show that p53 is able to suppress BNIP3 expression, thereby protecting cells against hypoxia-induced cell death [242]. In contrast, HIF-1α-mediated overexpression of BNIP3 in response to hypoxia is known to have a proapoptotic effect in human kidney epithelial cells [243]. Whether or not any, or all, of these genes contribute to susceptibility to OIR requires further investigation.

4.4.c.2 Strain-dependent differential expression of EGLN3 and EGLN1 in response to cyclic hyperoxia and the HIF-α oxygen sensing pathway

EGLN3 and EGLN1 belong to the prolyl hydroxylase family of oxygen-dependent enzymes which regulate expression of HIF-α by modification of the translated protein, and were chosen for further investigation as OIR is an oxygen-dependent disease [233]. Hydroxylation of specific proline residues in HIF-α by these prolyl hydroxylases mediates the binding of the tumour suppressor von Hippel-Lindau protein to target HIF-α for polyubiquitinylation and proteasomal degradation [52, 53]. Proline hydroxylation is the main mechanism by which HIF-α levels are regulated in response to hypoxia [35].

There are three members of the prolyl hydroxylase family: PHD1 (EGLN2), PHD2 (EGLN1), and PHD3 (EGLN3), all of which have been shown to have

different functions in regulating HIF-1α and HIF-2α [54]. Variation in the expression of prolyl hydroxylases in different human cell lines exposed to normoxia showed the activity of each prolyl hydroxylase appeared to be dependent on the relative abundance of the other prolyl hydroxylases present under a specific set of conditions, adding to the complexity of HIF-α regulation [54].

EGLN3 has been shown to regulate HIF-2α to a greater extent than HIF-1α, whereas EGLN1 appeared to have a greater affinity for HIF-1α [54]. Studies of HIF-2α knockdown mice with OIR show an absence of neovascularization, eventually resulting in the degeneration of the neural layers of the retina due to poor vascularization [49]. The importance of HIF-2α in retinal angiogenesis has been supported by another study involving mice with only one functional HIF-2α gene, in which retinal neovascularization was reduced in response to cyclic-hyperoxia exposure, due in part to an absence of pro-angiogenesis factors required to promote an angiogenic response [48]. HIF-1α is also required for the VEGF-mediated angiogenic response to hypoxia, as endothelial cell-specific deletion of HIF-1α in mice resulted in defects in blood vessel growth [244].

EGLN1 has been found to be the most abundantly expressed prolyl hydroxylase in normoxic conditions in cell lines studied by Appelhoff et al. [54]. In hypoxic conditions, EGLN2 expression remained unchanged or

significantly decreased upon exposure to hypoxia depending on the cell line. EGLN1 and, in particular, EGLN3 were greatly increased in response to hypoxia [54]. EGLN3 and EGLN1 are known to contain a hypoxia response element, allowing its induction by hypoxia to occur by HIF-α [245, 246]. The ability of EGLN3 and EGLN1 to remain active under hypoxic conditions suggests they may play a role in the physiological regulation of HIF–α through a HIF-dependent negative feedback loop (Figure 4.32) [54, 247]. This negative feedback loop may prevent the accumulation of HIF-α in sustained hypoxia and result in faster degradation upon reoxygenation [247].

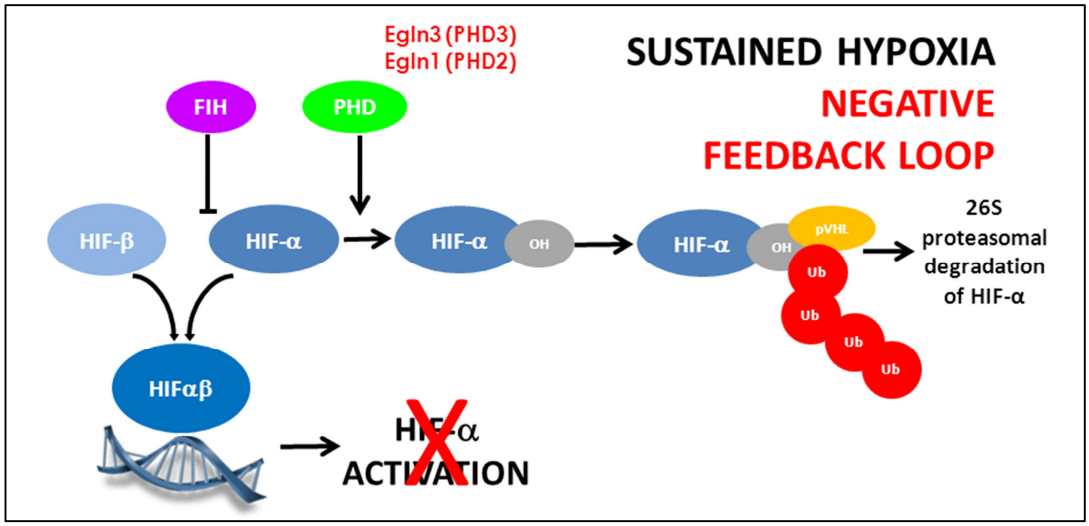

Figure 4.32 Simplified schematic representation of the HIF-α oxygen sensing pathway in sustained hypoxia. In conditions of sustained hypoxia, HIF-α is subject to a negative feedback loop as the oxygen-dependent prolyl hydroxylases (PHD) are able to remain active and hydroxylate HIF-α. This enables the von Hippel Lindau protein (pVHL) to bind to the hydroxylated HIF-α and target it for polyubiquitination and proteasomal degradation. Ub = Ubiquitin; PHD = Prolyl hydroxylase domain protein; FIH = Factor inhibiting HIF (Asparaginyl hydroxylase domain protein); pVHL = von Hippel Lindau protein.

Confirmation of Affymetrix microarray results in individual rats showed that EGLN3 appeared to be unchanged in response to hyperoxia at day 3 in F344 rats but was downregulated in SD rats (Figure 4.29). Large error bars in the F344 cyclic hyperoxia-exposed treatment group may be masking any effect of exposure to hyperoxia in these rats. At day 5, both strains showed downregulation of EGLN3 in response to hyperoxia. At day 6, EGLN3 was upregulated in resistant F344 rats but downregulated in susceptible SD rats. Expression of EGLN1 remained unchanged in response to hyperoxia at days 3 and 5 in both strains but by day 6, showed strain-dependent expression with an increase in EGLN1 observed in F344 rats and a decrease in expression seen in SD rats (Figure 4.30).

Increased expression of EGLN3 and EGLN1 in resistant F344 rats in response to relative hypoxia at day 6 may enable the prolyl hydroxylases to remain active in these conditions and negatively regulate HIF-α expression. In contrast, decreased expression of EGLN3 and EGLN1 in the susceptible SD rats suggests they are limited in their ability to regulate HIF-α expression in response to sustained hypoxia. This may allow HIF-α to accumulate and become activated, resulting in aberrant angiogenesis in the SD rats. Taken together, the ability of the prolyl hydroxylase (EGLN3/EGLN1) negative feedback loop to remain active at the critical time point of day 6 in resistant F344 rats, but not in susceptible SD rats, may be associated with strain-dependent differences in susceptibility to OIR.

The effects of changes in EGLN3 and EGLN1 expression on HIF-1α levels in the retina in response OIR are of interest, however, HIF-1α expression levels are difficult to determine. Under normoxic conditions, in this case represented by exposure to hyperoxia, HIF-1α is rapidly degraded by the ubiquitin proteasome pathway and has a half-life of less than 5 min [35, 248, 249]. The downstream processing of retinae in normoxia following removal of neonates from a hyperoxic environment takes 20–30 min; therefore the ability to accurately determine HIF-1α levels is not possible. Analysis changes in prolyl hydroxylase expression levels may potentially be used as a surrogate marker for HIF-1α in the context of OIR.

4.4.c.3 Strain-dependent differential expression of IGFBP3 in response to cyclic hyperoxia

IGF-1 is critical for normal foetal growth and development and plays a major role in normal vascularisation of the human retina [20, 224]. A study of premature infants has shown that a prolonged period of low IGF-1 levels in the plasma was associated with suppression of vascular growth which developed into proliferative ROP [250]. Early expression of high IGF-1 levels in premature infants results in increased retinal vascularisation and the absence of ROP. *In vitro*, IGF-1 has been shown to stimulate the accumulation of hypoxia-inducible factor-1α (HIF-1α) in human retinal pigment epithelial cells, resulting in increased VEGF mRNA expression [251]. IGF-1 has been found to regulate VEGF-induced endothelial cell survival through its

receptor IGF-1R [250, 252]. Low levels of IGF-1 and IGF-1R are associated with impaired retinal vascularisation in rodents [252].

Availability of IGF-1 in the body is regulated by a class of insulin-like growth factor binding proteins (IGFBPs) which bind to IGF-1 with high affinity and sequester the growth factor, limiting its activity [253]. There are 6 members of the IGFBP family (IGFBP-1 to IGFBP-6) which display distinct functional properties and have been shown to act both dependently and independently of IGF-1 [254]. Dysregulation of IGFBP expression has been reported in a variety of human disease such as cancer and proliferative retinopathies including OIR [255-257]. Monitoring serum IGF-1 and IGFBP3 levels has been suggested to provide some insight in identifying infants at high risk of developing severe disease and restoring levels may be a potential therapeutic strategy [236, 250, 258].

In a murine model of OIR, where mice were exposed to 5 days of sustained hyperoxia, followed by up to 21 days exposure to the relative hypoxia of room air, IGFBP2 expression remained unchanged between early and late time points in the exposure period [257]. Lofqvist and colleagues found that low levels of IGFBP3 were expressed at later time points during in the proliferative stages of OIR and were associated with persistent vaso-obliteration in the retina, whereas early expression was found to be protective against vessel loss [236]. On the other hand, IGFBP3 has also been

found to be upregulated 5 fold in response to hypoxia at day 17 in areas of the retina with neovascular tufts compared to normal vessels, suggesting it may have a role in vascular survival [257].

IGFBP2 and IGFBP3 were found to be downregulated in response to hyperoxia at day 3 by microarray analysis. Time-course analysis of IGFBP3 expression (Figure 4.31) showed its expression was relatively unchanged across all time points in resistant F344 rats, whereas it was downregulated in response to cyclic hyperoxia in SD rats. Stable expression of IGFBP3 in early OIR may be enough to provide some protection again hyperoxia-induced vessel loss in the resistant F344 rats, consistent with more advanced retinal vascularisation at all time points studied during the cyclic hyperoxia exposure period. The downregulation of IGFBP3 that is exhibited by susceptible SD rats may be consistent with the finding by Lofqvist that low levels of IGFBP3 expression in the proliferative stages of OIR are associated with persistent vaso-obliteration. This would be also consistent with the presence of large avascular areas in the retinae of SD rats susceptible to OIR, compared to the resistant F344 rats.

4.4.d CONCLUSION

Strain-dependent changes in retinal gene expression associated with prolyl hydroxylase regulation of the HIF-α oxygen sensing pathway and changes in IGFBP3 expression have been identified in early OIR. Significant differences

in the expression of EGLN3, EGLN1 and IGFBP3 were found to occur at day 6 in response to relative hypoxia in resistant F344 and susceptible SD rats which may underlie the differential susceptibility to OIR exhibited by these rat strains. The regulation of HIF-α by EGLN3 and EGLN1 has not previously been implicated in differential susceptibility to OIR and may be a potential therapeutic target for early intervention in ROP. Differences in IGFBP3 expression may contribute to susceptibility to OIR in SD rats and support existing findings that serum IGFBP3 levels could potentially be a used marker for disease progression in ROP. Taken together, this study has identified the differential regulation of three genes which may underlie differential susceptibility to OIR.